CHAPTER

3

Drug Release in Biological Tissues

Filippo de Monte[a], *Giuseppe Pontrelli*[b], *and Sid Becker*[c]

[a]Department of Industrial and Information Engineering and Economics, University of L'Aquila, L'Aquila, Italy,
[b]Istituto per le Applicazioni del Calcolo (IAC), CNR, Rome, Italy,
[c]University of Canterbury, Department of Mechanical Engineering, Christchurch, New Zealand

OUTLINE

http://dx.doi.org/10.1016/B978-0-12-415824-5.00003-5

Nomenclature

A	cross-sectional area (m^2)
Bi	Biot number
c	concentration $(kg\ m^{-3})$
$\langle c \rangle$	volume-averaged concentration $(kg\ m^{-3})$
D	effective diffusivity $(m^2\ s^{-1})$
f	retardation coefficient
G_X	One-dimensional Green function along $x (m^{-1})$
j	specific mass flux due to a concentration gradient $(kg\ s^{-1}\ m^{-2})$
$\hbar$	mass transfer coefficient $(m\ s^{-1})$
k	partition coefficient
K	porous medium permeability (m^2)
l	length (m)
m	mass (kg)
$\dot{m}$	mass flow rate $(kg\ s^{-1})$
M	mass per unita area $(kg\ m^{-2})$
p	pressure (Pa)
P	membrane permeability $(m\ s^{-1})$
Pe	Péclet number
r_h	hydraulic radius (m)
t	time (s)
u	velocity along $x (m\ s^{-1})$
V	volume (m^3)
x,y,z	Cartesian space coordinates (m)

Greek Symbols

β	reaction rate coefficient (s^{-1}). Also, β denotes eigenvalues in Subsection 3.5.1.
γ	diffusivity ratio

ε	volumetric porosity
ε_k	available volume fraction, $k\varepsilon$
λ	tortuosity. Also, λ denotes eigenvalues in Section 3.6.
μ	dynamic viscosity $(kg\ m^{-1}\ s^{-1})$
ρ	density $(kg\ m^{-3})$
σ	available volume fraction ratio
ϕ	dimensionless membrane permeability
Φ	Thiele Modulus

Acronyms

DES	Drug-Eluting Stent
EOS	Equation of State
LME	Local Mass Equilibrium
LMNE	Local Mass Non-Equilibrium
SOV	Separation of Variables

Subscripts

c	continuum
d	drug
rev	representative elementary volume

Superscripts

f	fluid phase
s	solid phase

3.1 INTRODUCTION

Problems involving the release of a drug from a polymeric gel matrix into biological tissues arise in a number of scientific and bioengineering disciplines. Important technological areas include drug-eluting stents for the prevention of restenosis [1–6], therapeutic contact lenses to increase the ocular bioavailability of ophthalmic drugs [7,8] and dermal and transdermal drug delivery [9–11].

The first application, concerning the process of restenosis after stent implantation for the treatment of coronary artery disease, is a result of a complex interplay of several implant-induced biological processes. Stent-based drug delivery has been shown to inhibit several of these biological processes, thereby preventing restenosis. A drug-eluting stent (DES) consists of a metallic stent platform with a polymeric coating that encapsulates a therapeutic drug, as shown in Fig. 3.1. Before the advent of DESs, stents were primarily used as scaffolds for keeping the arterial lumen opened, and their design involved interaction between vascular biology and engineering. As DES has come of age, the picture has become much more complex and multi-disciplinary. It now involves an interplay between vascular biology, polymer chemistry, pharmacology [1–4] and engineering [5,6]. In addition to being designed for structural integrity, deliverability to the lesion site and conformability with the arterial wall upon deployment, the stent also has to be optimized for drug delivery [3].

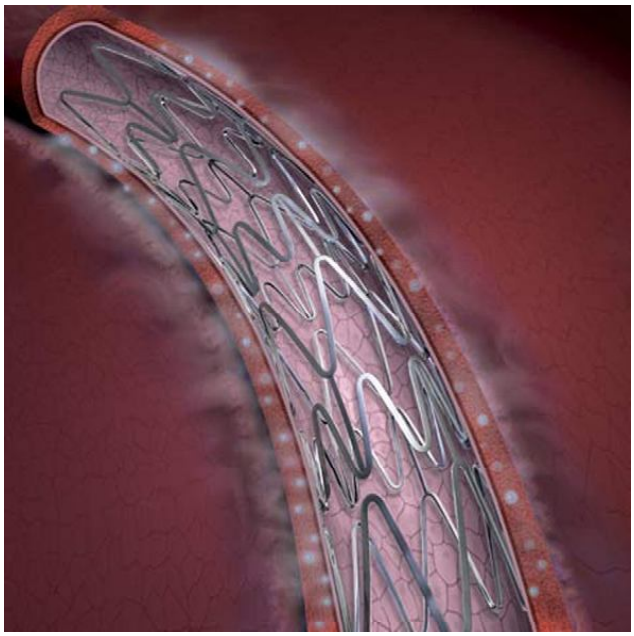

FIGURE 3.1 Drug-eluting coronary stent. It is coated with a drug that inhibits cell growth that could reclose a propped-open artery.

As far as the second application is concerned, diseases of the anterior segment of the eye are mostly treated by topical ocular administration in the inferior fornix of the conjunctiva. However, this procedure is extremely inefficient because when a drop (50 to 100 μl per drop) is instilled into the eye, the ophthalmic drug has a short residence time in the conjunctival sac of less than 5 min, and only 1–5% of the applied drug penetrates the cornea and reaches the intraocular tissues. The biovailability tends to be low and depends on the precorneal fluids dynamics, how well the drug binds to tear proteins, conjunctival drug absorption, tears turn over, resistance to corneal penetration, nasolachrymal drainage, metabolic degradation and non-productive absorption. The absorption and the efficacy of the instilled drug can be increased by altering its formulation and/or by changing the local conditions. For this reason, in recent years many researchers have proposed the use of therapeutic contact lenses to increase the ocular bioavailability of ophthalmic drugs [7] as illustrated in Fig. 3.2. The first attempt to increase the residence time of an ophthalmic drug involved the use of soaked contact lenses. The lens is hydrated and then placed onto the cornea where it releases the drug until an equilibrium is reached between drug concentration in the contact lens and that in the conjunctival sac. The maximum drug loading is limited by the solubility of the drug in the polymeric matrix and the delivery period of time is still very short. However, from a medical point of view, the central question is to be able to predict the concentration of the drug in the anterior chamber of the eye [8]. In this case, mathematical models and numerical simulations are the only available tools to make such predictions.

Transdermal drug delivery (Fig. 3.3) has made an important contribution to medical practice, but has still to fully achieve its potential as an alternative to oral delivery and hypodermic injections. While much time and effort have been devoted to understanding the Fickian principles of drug diffusion across the skin membrane, one area of research that has been neglected has been transfollicular drug delivery. First-generation transdermal delivery systems

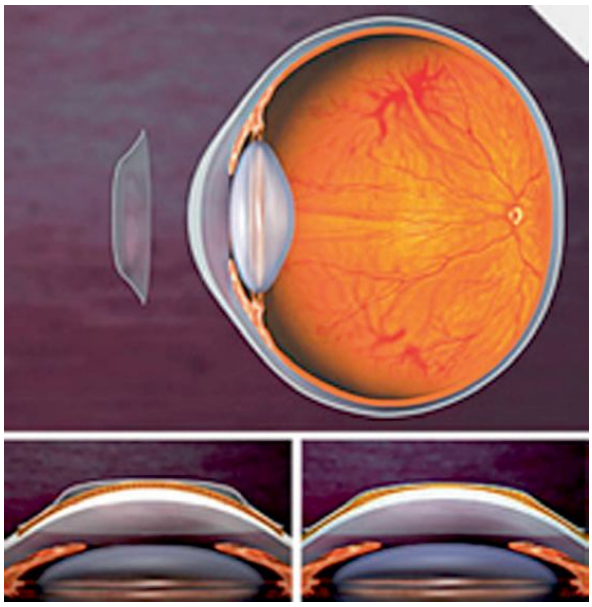

FIGURE 3.2 Therapeutic contact lens used for reshaping cornea and drug delivery.

FIGURE 3.3 A depiction of the composite nature of skin.

have continued their steady increase in the clinical, where they are used for the delivery of small, lipophilic, low-dose drugs. Second-generation delivery systems using chemical enhancers, noncavitational ultrasound and iontophoresis have also resulted in clinical products; the ability of iontophoresis to control delivery rates in real time provides added functionality. Third-generation delivery systems target their effects to the skin's barrier layer, the stratum corneum, using microneedles, thermal ablation, microdermabrasion, electroporation and

cavitational ultrasound. Microneedles and thermal ablation are currently progressing through clinical trials for delivery of macromolecules and vaccines, such as insulin, parathyroid hormone and influenza vaccine. Using these novel second- and third-generation enhancement strategies, transdermal delivery is poised to significantly increase its impact on medicine [10].

Several studies address the modeling of transdermal diffusion of drugs to better understand the permeation of molecules through the skin, especially the stratum corneum, which forms the main permeation barrier to percutaneous permeation [9]. In order to ensure the reproducibility and predictability of drug permeation through the skin and into the body, a quantitative understanding of the permeation barrier properties of the stratum corneum is crucial. Multiscale frameworks for modeling the multicomponent transdermal diffusion of molecules have been proposed in the literature [11]. The problem is in general divided into smaller problems of increasing length scale: microscopic, mesoscopic and macroscopic. First, the microscopic diffusion coefficient in the lipid bilayers of the stratum corneum is found through molecular dynamics (MD) simulations. Then, a homogenization procedure is performed over a model unit cell of the heterogeneous stratum corneum, resulting in effective diffusion parameters. These effective parameters are the macroscopic diffusion coefficients for the homogeneous medium that is 'equivalent' to the heterogeneous stratum corneum, and thus can be used in finite element simulations of the macroscopic diffusion process.

All these applications share the same modeling framework: the delivery of a drug from a polymeric matrix in contact with a biological tissue for therapeutic purposes. Such a tissue can be treated as a porous medium [12] as it is composed of dispersed cells separated by connective voids which allow nutrients, drugs, minerals, etc. to reach all cells within the tissue. Mass transport of these substances in many biological and medical applications is achieved by advection and diffusion within the tissue which may be enhanced by interstitial flows. Polymeric gels can be treated as porous media too. To obtain a sound understanding of the drug delivery process, mathematical modeling can be divided into two categories, as follows:

1. modeling of drug elution from the polymeric gel; and
2. modeling of transport of the drug in the biological tissue.

Both these models provide valuable insights to the engineers and scientists to assist in the design of drug delivery systems. They are strictly coupled, and can help the system designer to achieve a particular release rate and release time, as well a desired drug distribution and tissue concentration. For modeling purposes, it is important to identify the dominant physicochemical processes by the relevant parameters and take them into account when developing the mathematical model (see Sections 3.2 and 3.3). For example, in the coating of DESs, we have two phases (solid and fluid) whose drug concentrations are different, so generating the so-called *local mass non-equilibrium* (LMNE) involves a complex and challenging mathematical treatment [13] (see Section 3.4). However, the simplifying assumption of *local mass equilibrium* (LME) can sometimes be used [14] and this is detailed in Section 3.5. Only one phase, the fluid phase, will be considered when the drug diffuses within biological tissues.

In the second part of this chapter (Section 3.6), DES application has been selected to show the use of a hierarchy of models of increasing complexity. The first subsection 3.6.1 considers the fluid wall model for the arterial wall by using the Pure Diffusion Approximation. Then, this is extended in the second subsection 3.6.2 by making use of the Diffusion-Reaction-Advection Equation. Finally, the third subsection 3.6.3 shows the multi-layered wall model for the artery by again applying the Pure Diffusion Approximation.

3.2 CONTINUUM MODELING OF MASS TRANSPORT IN POROUS MEDIA

Consider a porous medium whose fluid and solid phases are binary mixtures, that is, mixtures of only two components; for example, when a DES is considered, these are drug (solute) and plasma (solvent) for the fluid phase, and drug (solute) and polymeric gel (solvent) for the solid phase.

To describe the mass transport of drug in each of these two phases, two different scales, microscopic and macroscopic (continuum), may be used. In the microscopic approach, the typical microscopic governing equations have to be written for each phase and then solved, either numerically or analytically. Specifically, for each phase the physics are captured by:

- the fluid phase: continuity and momentum equations, conservation of drug mass, boundary and initial conditions;
- the solid phase: conservation of drug mass and related boundary and initial conditions.

This approach allows the drug concentration in both phases to be derived as a function of the space and time coordinates. These concentrations are defined as:

$$C_d^f \triangleq \frac{dm_d^f}{dV^f}, \quad C_d^s \triangleq \frac{dm_d^s}{dV^s} \tag{3.1a}$$

$$dm_d^f \text{ and } dm_d^s \tag{3.1b}$$

where dV^f and dV^s are the elemental masses of drug contained into the fluid and solid elemental volumes c_d^f, respectively, as shown in Fig. 3.4.

Note also that c_d^f depends on $(x^f, y^f, z^f) \in V^f$, where x^f, y^f and $z^f \in V^f$ are the Cartesian coordinates of a point P^f within the fluid phase. Similarly, c_d^s depends on $(x^s, y^s, z^s) \in V^s$, where x^s, y^s and z^s are the space coordinates of a point P^s in the solid phase.

The microscopic approach, however, requires knowledge of the specific and local geometric shape of the individual pore structure networks, but these are in general not known. This is the motivation behind the continuum approach, which assumes that a porous medium may be represented as a globally homogeneous material by appropriately defining average variables over a sufficiently large volume, 'representative elementary volume' (r.e.v., for short), as depicted in Fig. 3.4. Hence, when dealing with the continuum approach (macroscopic), an elemental volume dV_c (where the subscript c denotes continuum) is greater than V_{rev}.

The length scale l of the r.e.v. is much larger than the pore scale given by the average size δ of the pores, but considerably smaller than the length scale L over which macroscopic changes of physical quantities, such as drug concentration and fluid velocity, have to be considered. Hence, the continuum approach requires that $\delta \ll l \ll L \Rightarrow L$ has to be at least two orders of magnitude larger than δ as in Section 8.3 of Ref. [15]. In biological tissues, it happens that $\delta < 0.1\ \mu m, l \sim 1\ \mu m,$ and $L \sim 10\ \mu m$ to 1 cm, where L is chosen to be the characteristic linear dimension of the biological medium, for example the size of tissues or the distance between adjacent blood vessels. As a matter of fact, typical values found in the literature for the geometrical dimensions of arteries indicate a thickness L of only 2 μm for endothelium and IEL layers, but in this case the average size δ of the pores can be considered sufficiently less than

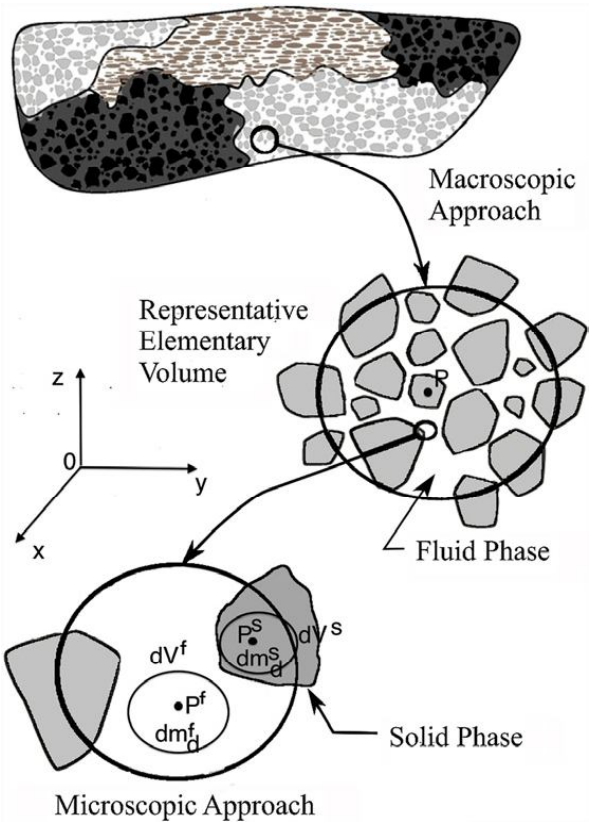

FIGURE 3.4 Schematic of the main scales in a porous medium with the representative elementary volume (r.e.v.).

0.1 μm. In the polymeric gel coating of DESs, $\delta < 0.1\ \mu m$ and $L \sim 5\ \mu m$ [5]. Therefore, solute transport in coatings and biological tissues can be analyzed by using the continuum approach.

When the continuum modeling is used, the details of the pore structures are neglected and macroscopic geometrical and physical variables, such as porosity, permeability and tortuosity, have to be defined. The porosity is strictly geometrical and is defined in Section 3.2.1 alongside the volume-averaged variables. The permeability appears in the momentum equation, and when the inertial contributions are negligible, it provides a linear relationship between pressure drop and flow rate, as indicated by the Darcy law (Section 3.2.2). Finally, Fick's law still applies for diffusion in porous media but is affected by another strictly geometrical variable, the tortuosity, as discussed in Section 3.2.3.

3.2.1 Porosity and Volume-Averaged Variables

The porosity ε (dimensionless), also called the 'volumetric' porosity, is the ratio of the void volume V^f contained in the porous medium and occupied by the fluid to the total volume V of the same medium. We have:

$$\varepsilon = \frac{V^f}{V} = \frac{V^f}{V^f + V^s} \tag{3.2}$$

(less than 1) where V^s is the volume of the solid part, represented by biological cells or polymeric matrix of the coating, as displayed in Fig. 3.1.

The porosity does not give any information about the interconnectedness of the void (the pores). In general pores may be penetrable or isolated, where the penetrable pores can be further classified as either passing or nonpassing as in Section 8.2 of Ref. [15]. Nonpassing pores can be considered as part of the solid matrix when dealing with transport analysis and an 'effective' porosity (ratio of connected void to total volume) can likely be introduced.

In fluid-saturated porous media (of interest in this chapter) that can be modeled as nondeformable, homogeneous, and isotropic, the volumetric porosity ε is the same as the so-called 'surface' porosity; that is, the fraction of void area (or free-flow area, A^f) to total area A of a typical cross section [16,17]. Hence, in these porous structures, all the void volume is connected; that is, all the pores are penetrable and passing.

It is relevant to observe that not all the penetrable and passing pores are accessible to solutes. In fact, it can happen that a pore is inaccessible to a solute if the solute molecule is larger than the pore, or if the pore is large enough but is surrounded by pores that are smaller than the solutes. The portion of void volume that is accessible to a solute is called 'available volume'. The ratio of the available volume to the void volume is defined as the 'partition coefficient' of the solute and is denoted by $k(\leq 1)$. Then, the product of k and ε is defined as the 'available volume fraction' ε_k, which provides the ratio of the available volume to the total volume of the porous structure, with $\varepsilon_k \leq \varepsilon$.

3.2.1.1 *Averaged Concentration*

There are two different ways of averaging over a volume. One is based on the volume of each phase contained in r.e.v., that is, V^f_{rev} for the fluid phase (which is a portion of the r.e.v., i.e., ε) and V^s_{rev} for the solid phase (which is the complementary portion of the r.e.v., i.e., $1-\varepsilon$). Another is based on the total volume of the r.e.v. (incorporating both fluid and solid material), given by $V_{rev} = V^f_{rev} + V^s_{rev}$.

For example, we can take a volume average of c^f_d as defined by Eq. (3.1a) with respect to the corresponding phase volume or over the total volume (r.e.v.). Thus we have, respectively,

$$\left\langle c^f_d \right\rangle^f \triangleq \frac{1}{V^f_{rev}} \underbrace{\int_{V^f_{rev}} c^f_d \, dV^f_{rev}}_{m^f_d} \tag{3.3a}$$

$$\left\langle c^f_d \right\rangle \triangleq \frac{1}{V_{rev}} \int_{V_{rev}} c^f_d \, dV_{rev} = \frac{1}{V_{rev}} \underbrace{\int_{V^f_{rev}} c^f_d \, dV^f_{rev}}_{m^f_d} \tag{3.3b}$$

where $\left\langle c^f_d \right\rangle$ and $\left\langle c^f_d \right\rangle^f$ depend on x, y and z, which are the Cartesian coordinates of the centroid P of the r.e.v. (see Fig. 3.4), and m^f_d is the mass of drug contained in the fluid phase volume V^f_{rev}.

Equation (3.3a) gives the so-called intrinsic volume-averaged concentration of c^f_d, while Eq. (3.3b) yields its volume-averaged concentration [13,14,17]. Comparing the above two equations yields $\left\langle c^f_d \right\rangle = \varepsilon \left\langle c^f_d \right\rangle^f$. In addition, if not all the penetrable and passing pores are

accessible to the drug, we have $\left\langle c_d^f \right\rangle = \varepsilon_k \left\langle c_d^f \right\rangle^f$. Also, the averaging operation of c_d^f performed through the above integrals provides the value of the drug concentration in the fluid phase at the centroid P, which can fall in the fluid or solid phase. In the case of Fig. 3.4, it falls in the solid phase. Also, it is assumed that the result of averaging over a volume is independent of the size of the r.e.v.

Similarly, we can take an average of c_d^s with respect to the solid phase volume V_{rev}^s (intrinsic average) or over the total volume V_{rev}. We obtain, respectively,

$$\left\langle c_d^s \right\rangle^s \triangleq \frac{1}{V_{rev}^s} \underbrace{\int_{V_{rev}^s} c_d^s \, dV_{rev}^s}_{m_d^s} \tag{3.4a}$$

$$\left\langle c_d^s \right\rangle \triangleq \frac{1}{V_{rev}} \int_{V_{rev}} c_d^s \, dV_{rev} = \frac{1}{V_{rev}} \underbrace{\int_{V_{rev}^s} c_d^s \, dV_{rev}^s}_{m_d^s} \tag{3.4b}$$

where $\left\langle c_d^s \right\rangle$ and $\left\langle c_d^s \right\rangle^s$ depend on x, y and z and m_d^s is the mass of drug contained in the solid phase of volume V_{rev}^s. Also, $\left\langle c_d^s \right\rangle = (1-\varepsilon)\left\langle c_d^s \right\rangle^s$, or $\left\langle c_d^s \right\rangle = (1-\varepsilon_k)\left\langle c_d^s \right\rangle^s$.

The averaging operation of c_d^s yields the value of drug concentration in the solid phase at the centroid P of the r.e.v., where a drug concentration in the fluid phase also exists. Therefore, each spatial point of the porous medium simultaneously contains two phases: a fluid phase with a volume fraction of ε (or ε_k) and a solid phase with a volume fraction of $1-\varepsilon$ (or $1-\varepsilon_k$). Similarly, we can get the spatial average of other variables involved in the mass transport phenomenon, such as fluid velocity, pressure, temperature and so on.

3.2.2 Permeability, Darcy's Law and the Continuity Equation

The permeability K is a measure of the flow conductivity in the porous medium. In flows for which the viscous effects dominate the inertial interactions (very low Reynolds number, probably around 5), the pressure gradient and the flow rate are linearly related. This flow regime is characteristic of many transport mechanisms in biological media. The permeability appears in Darcy's law (which is a derivation of the momentum balance in porous media) as the constant of linearity between the average flow velocity u and the pressure gradient (driving potential). In one dimension along x, Darcy model is expressed by

$$u = -\frac{K}{\mu}\frac{\partial p}{\partial x} \tag{3.5}$$

where p and μ are the fluid pressure and dynamic viscosity, respectively. The permeability has dimensions of (length)^2 and depends only on the geometry of the medium. The ratio K/μ is defined as the 'hydraulic conductivity'; for this reason, the permeability K is also called the 'specific hydraulic permeability'.

As the Darcy model ignores boundary effects on the flow, advanced models such as Forchheimer's equation and Brinkman's equation are available in the porous medium literature.

The former is applicable for large flow velocities, while the latter accounts for the boundary effects. The reader may refer to the studies [12] in Section 8.3 of Ref. [15] and Section 1.5 of Ref. [17].

The flow velocity u appearing in Eq. (3.5) is actually a spatial averaged velocity taken with respect to the total volume (r.e.v.), that is, $\langle u \rangle$. In general it depends on the space x and time t coordinates, and is termed the 'Darcy velocity', though various names are also used in the literature, such as filtration velocity or seepage velocity [16,17]. This velocity is related to the intrinsic volume-averaged velocity $\langle u \rangle^f$ through the Dupuit-Forchheimer relationship, $\langle u \rangle = \varepsilon \langle u \rangle^f$ [16]. We may also have $\langle u \rangle = \varepsilon_k \langle u \rangle^f$.

It is relevant to note that in the Darcy model, Eq. (3.5), u (effect) is an average velocity over the total volume, while p in the pressure gradient (cause) is an 'intrinsic' quantity, that is, a quantity whose average is based on the fluid phase volume, $\langle p \rangle^f$. For the sake of simplicity and brevity, in this chapter we will use u, u^f and p in place of, $\langle u \rangle, \langle u \rangle^f$ and $\langle p \rangle^f$, respectively.

Then, as we have two unknowns, u and p, and only Darcy's law, we need another equation to close the system. We can make use of the conservation of fluid mass in one dimension along x, as indicated in the next two subsections.

3.2.2.1 *The Continuity Equation*

Consider a 1-D differential volume element in the macroscopic flow field, $dV_c^f = A^f dx$, as depicted in Fig. 3.5. It is greater than V_{rev}^f and, hence, other than dV^f of Fig. 3.4 and Eq. (3.1a) related to the microscopic approach. Writing a mass balance for this elemental volume yields the continuity equation along x. This balance may be stated as:

$$\begin{pmatrix}\text{net rate of mass flow entering}\\ \text{volume element in } x \text{ direction}\end{pmatrix} = \begin{pmatrix}\text{rate of increase of the fluid}\\ \text{mass in volume element}\end{pmatrix} \tag{3.6}$$

Both terms in the above statement can be evaluated as follows.

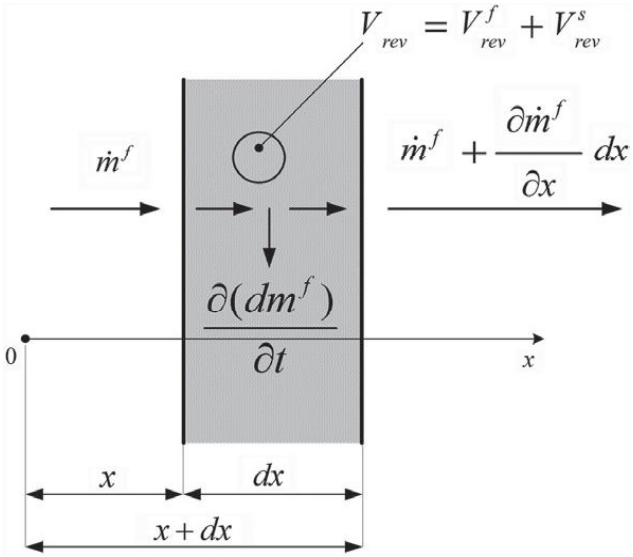

FIGURE 3.5 Nomenclature for the derivation of the continuity equation in a porous medium using the continuum approach.

First, let ρ^f be the fluid density, which in general depends on both temperature and pressure. It is defined as dm^f/dV_c^f, where dm^f is the elemental fluid mass contained into the fluid elemental volume dV_c^f. If $\dot{m}^f = \rho^f u^f A^f$ is the mass flow rate into the element in the x direction through the cross-sectional free-flow area A^f at x, then $\dot{m}^f + (\partial \dot{m}^f/\partial x)dx$ is the mass flow rate leaving the element along the same x direction through the surface A^f at $x + dx$. The net rate of mass flow into the element is the difference between the entering and leaving flow rates, given by:

$$\begin{pmatrix}\text{net rate of mass flow entering}\\ \text{volume element in } x \text{ direction}\end{pmatrix} = -\frac{\partial \dot{m}^f}{\partial x}dx = -A^f \frac{\partial(\rho^f u^f)}{\partial x}dx \tag{3.7}$$

noting that A^f is independent of x.

Second, the fluid mass content dm^f of the volume element dV_c^f is $\rho^f A^f dx$. Then, the rate of increase of this mass content is obtained by taking its partial derivative with respect to time, that is, $[\partial(\rho^f A^f)/\partial t]dx$. Therefore, we can write:

$$\begin{pmatrix}\text{rate of increase of the fluid}\\ \text{mass in volume element}\end{pmatrix} = A^f \frac{\partial \rho^f}{\partial t}dx \tag{3.8}$$

noting that A^f is also independent of t.

Substituting Eqs. (3.7) and (3.8) into Eq. (3.6), we obtain the continuity equation at a macroscopic level (continuum approach):

$$\varepsilon_k \frac{\partial \rho^f}{\partial t} + \frac{\partial(\rho^f u)}{\partial x} = 0 \tag{3.9}$$

where we have used $u^f = u/\varepsilon_k$, that is, $\langle u \rangle^f = \langle u \rangle / \varepsilon_k$; also, the fluid density ρ^f is an 'intrinsic' quantity, i.e., $\langle \rho^f \rangle^f$, and is related to the fluid pressure p appearing in Eq. (3.5) through the equation of state (EOS) of the fluid under consideration. For instance, for an ideal gas, we have $\rho^f = p/RT^f$, where T^f is the 'intrinsic' volume-averaged gas temperature, i.e., $\langle T^f \rangle^f$, and R its characteristic constant. If T^f is also unknown, we need another equation, that is, the conservation-of-energy equation in the fluid phase, as indicated in Section 3.3.3.

Note that the continuity equation defined by Eq. (3.9) is valid for pure fluids. If the fluid that saturates the porous structure is a mixture of two or more chemical species, for example drug (solute) and plasma (solvent), the fluid density ρ^f is the fluid mixture density. Also, u^f refers to the fluid velocity that is in general different from the velocities of either chemical species contained in the fluid (see Section 3.3.1).

Alternatively, Eq. (3.9) can be obtained by first writing the microscopic continuity equation for the fluid phase and, then by integrating it over the total volume V_{rev}. When integrating it, well-established theorems such as the transport and averaging theorems have to be properly used, as shown in [13] and Section 3.5 of Ref. [17].

Equations (3.5) and (3.9), along with the initial and boundary conditions for fluid velocity and pressure, are the governing equations for the transient, one-dimensional flow of a fluid through a porous medium. For an incompressible, isothermal fluid, ρ^f is uniform and constant, and Eq. (3.9) reduces to $\partial u/\partial x = 0 \Rightarrow u$ is independent of the space coordinate x.

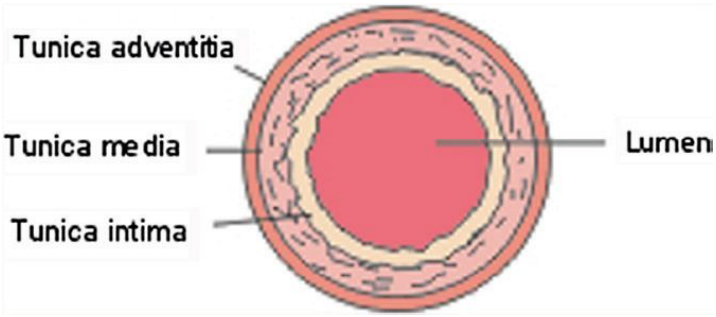

FIGURE 3.6 A normal elastic artery. The walls of arteries are composed of three main concentric zones: Tunica adventitia (outer), tunica media (middle), and tunica intima (inner layer).

Then, integrating the Darcy model given by Eq. (3.5) between $x = 0$ (pressure p_1) and $x = l$ (pressure p_2) yields the following simple velocity profile:

$$u = \frac{p_1 - p_2}{\mu l / K} \tag{3.10}$$

Hence, the velocity is proportional to the applied pressure difference and inversely proportional to the quantity $\mu l/K$, which may be seen as a hydraulic resistance to the fluid flow. In human medium sized arteries (see Fig. 3.6), the pressure difference between lumen and adventitia, under normal conditions, does not exceed 100 mmHg. As $K = 2 \cdot 10^{-14}\ cm^2$ represents the average permeability of an arterial wall with a thickness of 220 μm, and $\mu = 0.72 \cdot 10^{-2}\ g\ cm^{-1}\ s^{-1}$ is the viscosity of plasma, the magnitude of the Darcy velocity given by Eq. (3.10) is about 10^{-6} cm s^{-1}.

It is important to observe that Eq. (3.9) is valid if there is no fluid production (source) or fluid consumption (sink) in the medium. However, sources and sinks can be present in biological (porous) tissues because of fluid exchanges between the interstitial space and the blood or lymph vessels, as discussed in next section.

3.2.2.2 *Extended Continuity Equation*

An extension of Eq. (3.7) for biological media is:

$$\begin{pmatrix}\text{net rate of mass flow entering}\\ \text{volume element in } x \text{ direction}\end{pmatrix} + \begin{pmatrix}\text{fluid mass rate produced}\\ \text{into the elemental volume}\end{pmatrix} - \begin{pmatrix}\text{fluid mass rate consumed}\\ \text{into the elemental volume}\end{pmatrix} = \begin{pmatrix}\text{rate of increase of the fluid}\\ \text{mass in volume element}\end{pmatrix} \tag{3.11}$$

If $g_b^f = d\dot{m}_b^f / dV^f$ is the rate of mass fluid flow per unit volume of fluid phase from blood vessels into the interstitial fluid space (units of $kg\ s^{-1}\ m^{-3}$), we have:

$$\begin{pmatrix}\text{fluid mass rate produced}\\ \text{into the elemental volume}\end{pmatrix} = g_b^f A^f dx \tag{3.12}$$

Similarly, if $g_l^f = d\dot{m}_l^f / dV^f$ is the rate of mass fluid flow per unit volume of fluid phase from the interstitial fluid space into lymph vessels (in $kg\ s^{-1}\ m^{-3}$), we can write:

$$\begin{pmatrix}\text{fluid mass rate consumed}\\ \text{into the elemental volume}\end{pmatrix} = g_l^f A^f dx \tag{3.13}$$

Substituting Eqs. (3.7), (3.8), (3.12) and (3.13) into Eq. (3.11), after some algebraic manipulation, we get:

$$\varepsilon_k \frac{\partial \rho^f}{\partial t} + \frac{\partial (\rho^f u)}{\partial x} = \varepsilon_k g_b^f - \varepsilon_k g_l^f \tag{3.14}$$

where the subscripts b and l refer to the blood and lymph vessels, respectively.

We recall that, in the above equation, ρ^f, g_b^f and g_l^f are average quantities per unit volume of the fluid phase, whereas u is an average quantity per unit volume of the biological tissue (porous medium). For an incompressible, isothermal fluid, this equation reduces to:

$$\frac{\partial u}{\partial x} = \varepsilon_k \left(g_b^f\right)' - \varepsilon_k \left(g_l^f\right)' \tag{3.15}$$

where $(g_b^f)'$ and $(g_l^f)'$ are the rates of volumetric fluid flow per unit volume of fluid phase, respectively. Their values are determined by using Starling's law (see Chap. 9 of Ref. [15]).

3.2.3 Tortuosity and Fick's Law

The tortuosity, λ, is an important characteristic for the combination of the fluid and the geometry of the porous medium. It accounts for the motion of fluid molecules that follow tortuous pathways in the void space and is defined on p. 430 of Ref. [15] as:

$$\lambda = \left(\frac{L_{\min}}{L}\right)^2 \tag{3.16}$$

where $L_{\min}$ is the shortest path length (measured through connected pores) between any two points of the fluid in a porous medium, and L is the straight-line distance between the same two points.

Equation (3.16) states that the tortuosity is dimensionless, and is always greater than or equal to unity. Along with other factors, it affects the solute transport by diffusion in porous media. Within the fluid and solid phases of the porous structure Fick's law still applies for diffusion, but the diffusivity has to be appropriately revisited in order to account for the tortuosity. For this purpose, we recall that for a binary fluid mixture of two components, for example drug (solute) and plasma (solvent), Fick's model is expressed, in the absence of the porous medium and in one dimension (along x), by:

$$j_d^f = -D_{d0}^f \frac{\partial c_d^f}{\partial x} \tag{3.17}$$

where j_d^f is the mass flux of drug per unit area in the fluid binary mixture (superscript f). Also, D_{d0}^f is the diffusivity or diffusion coefficient of the drug in the same fluid mixture, where the subscript 0 denotes the absence of the porous medium.

Hence, Fick's equation linearly relates the drug mass flux by diffusion to the concentration gradient (driving potential) through a physical property called the diffusivity. In the presence of the porous structure, Eq. (3.17) is still valid, but the diffusion of solute is characterized by the so-called 'effective' diffusivity or 'effective' diffusion coefficient, D_d^f. This is related to the former, D_{d0}^f, through the tortuosity of pathways for diffusion and an additional viscosity function f_η accounting for local boundaries and local viscosity as follows [12]:

$$D_d^f = \frac{D_{d0}^f}{(\lambda f_\eta)^2} \tag{3.18}$$

where D_d^f is less than D_{d0}^f.

The quantity $(\lambda f_\eta)^2$ represents the hindrance to 'flow diffusion' inside the pores. As the tortuosity generally increases with a decrease in porosity, a decrease in the latter significantly reduces the effective mass diffusivity of a drug in the fluid mixture, and hence, the drug flux j_d^f.

When applying Fick's model to the fluid phase of a porous medium, we use the local concentration c_d^f, as defined by Eq. (3.1a), provided a microscopic approach is used. But if the treatment deals with a continuum approach (see Section 3.2), we have to account for a volume-averaged concentration of drug at point x and time t. This average is to be taken over the volume occupied by the fluid, as indicated by Eq. (3.3a). Hence, the term c_d^f appearing in Eq. (3.17) is actually $\langle c_d^f \rangle^f = \langle c_d^f \rangle / \varepsilon_k$, where $\langle c_d^f \rangle$ is defined by Eq. (3.3b). Also, the effective diffusivity D_d^f of Eq. (3.18) is averaged over the volume of the fluid phase, that is, $\langle D_d^f \rangle^f = \langle D_d^f \rangle / \varepsilon_k$, where $\langle D_d^f \rangle$ is averaged over the total volume (r.e.v.).

Similarly, when the solid phase of the porous structure is a binary mixture, we can apply Fick's model. In one dimension (along x), it is given by:

$$j_d^s = -D_d^s \frac{\partial c_d^s}{\partial x} \tag{3.19}$$

where j_d^s is the flux of drug per unit area in the solid binary mixture, c_d^s is an intrinsic volume-averaged concentration as defined by Eq. (3.4a), i.e., $\langle c_d^s \rangle^s = \langle c_d^s \rangle / (1 - \varepsilon_k)$, and D_d^s is the 'effective' diffusivity of the drug in the solid mixture averaged over the solid phase volume, namely $\langle D_d^s \rangle^s = \langle D_d^s \rangle / (1 - \varepsilon_k)$. Then, in some way D_d^s is related to the diffusivity D_{d0}^s in absence of the porous structure.

3.3 CONSERVATION OF DRUG MASS

The fluid that saturates the porous structure can be a mixture of two or more chemical species. For the purposes of this chapter, it suffices to consider a binary mixture of only two chemical species; one being the plasma and the other being the drug. However, as the

concentration of the drug is several orders of magnitude less than that of plasma, our attention focuses only on the transport of the drug.

In addition, as the drug can also be contained in the solid phase of the porous medium, such as in the coating of DESs or therapeutic contact lenses, a rigorous analysis of mass transfer involves solving two coupled partial differential equations expressing the conservation of drug mass, one for the fluid and the other for the porous material, which represent the so-called fluid and solid phases, respectively.

In this case, the porous material gives up the drug to the fluid flowing through it when its concentration in the fluid phase c_d^f is less than that c_d^s in the solid phase. This model may be denoted as 'two-phase model', and must not be confused with the well-known notation of 'two-phase flow' (or 'two-phase fluid flow'), which indicates that two miscible fluids (a liquid and a gas, or two liquids/gases) share the void volume of the porous structure [17]. In the current case, the void is saturated by a single fluid ('single-phase flow'), which is a mixture of two components.

As there are two coupled partial differential equations expressing the drug conservation, one in the fluid phase and the other in the solid phase, the solution will be represented by two concentration functions of the same substance, c_d^f and c_d^s, respectively, which are intrinsic volume-averaged concentrations.

3.3.1 Drug Mass Balance in the Fluid Phase

Let us assume a one-dimensional (1-D) model where the fluid containing the substance of interest flows uniformly with velocity u^f in the direction of the x axis, which in general depends on the space x and time t coordinates. The fluid is supposed to be well mixed, so that the concentration of the only substance can be considered uniform in any plane perpendicular to the direction of flow.

The concentration distribution $c_d^f(x,t)$ in the fluid flow field is governed by the conservation of drug mass, which can be derived by writing a drug mass balance for a 1-D differential volume element in the flow field, $dV_c^f = A^f dx$, as shown in Fig. 3.7. This balance may be stated as:

$$\begin{aligned}&\begin{pmatrix}\text{net rate of drug mass}\\ \text{entering volume element}\end{pmatrix}+\begin{pmatrix}\text{net rate of drug mass diffusion}\\ \text{into the elemental volume}\end{pmatrix}\\&+\begin{pmatrix}\text{drug consumption}\\ \text{rate in element}\end{pmatrix}+\begin{pmatrix}\text{drug mass rate produced by chemical}\\ \text{reaction into the elemental volume}\end{pmatrix}\\&+\begin{pmatrix}\text{mass transfer rate of}\\ \text{drug with solid-phase}\end{pmatrix}=\begin{pmatrix}\text{rate of increase of drug}\\ \text{mass in element}\end{pmatrix}\end{aligned}\tag{3.20}$$

Each term in the above statement can be evaluated as given in the following paragraphs. The fluid flowing through the porous medium is considered a constant property. First, let u_d^f be the drug (solute) velocity in the fluid plasma (solvent), which is not necessarily equal to solvent velocity u_p^f (the subscript p denotes plasma). Solutes are actually more hindered by porous structures than solvents are. This phenomenon is taken into account by the so-called 'retardation coefficient', f, which expresses the ratio of the drug (solute) velocity u_d^f in the fluid to the solvent velocity u_p^f (this coefficient is paid little attention in biological tissues). If we

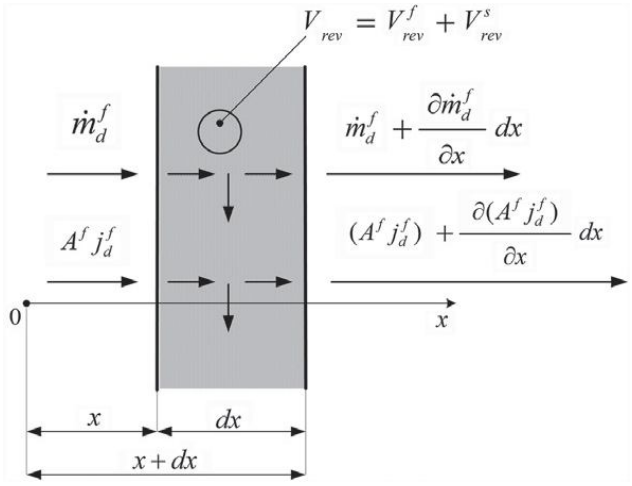

FIGURE 3.7 Nomenclature for the derivation of the drug balance equation in the fluid phase of a porous medium.

assume that the solvent velocity is equal to the fluid velocity, u^f, we can write $f = u^f_d/u^f$ (with the value of f being between zero and unity). This assumption is reasonable in dilute systems since, in these systems, the fluid velocity u^f may be considered independent of the solute concentration and, hence, can be derived independently, using the momentum and continuity equations given in Section 3.2.2.

Then, if $\dot{m}^f_d = c^f_d u^f_d A^f$ is the drug mass flux into the element in the x direction through the cross-sectional free-flow area A^f at x, then $\dot{m}^f_d + (\partial \dot{m}^f_d/\partial x)dx$ is the rate of drug mass flow leaving the element along the same x direction through the surface at $x + dx$. The net rate of drug mass into the element is the difference between the entering and leaving flow rates, given by:

$$\begin{pmatrix} \text{net rate of drug mass} \\ \text{entering volume element} \end{pmatrix} = -\frac{\partial \dot{m}^f_d}{\partial x} dx = -A^f \frac{\partial (f u^f c^f_d)}{\partial x} dx \tag{3.21}$$

where we have assumed that $u^f_p \approx u^f$, as for dilute systems, and noting that A^f is independent of x.

Equation (3.21) says that the convective (or advective) transport of a drug across the tissue is due to its velocity $u^f_d \approx f u^f$, where f accounts for the reduction of the convective influence due to the collisions of large molecules of drug with the solid matrix of the porous structure. We also recall that the flow velocity u^f is related to the Darcy velocity u through the relationship $u^f = u/(k\varepsilon)$.

Second, referring to the nomenclature shown in Fig. 3.7, the diffusion contribution is represented by:

$$\begin{pmatrix} \text{net rate of drug mass diffusion} \\ \text{into the elemental volume} \end{pmatrix} = -\frac{\partial (A^f j^f_d)}{\partial x} dx = A^f D^f_d \frac{\partial^2 c^f_d}{\partial x^2} dx \tag{3.22}$$

for which the diffusive flux of drug j^f_d per unit free-flow area A^f is given by Fick's law (see Section 3.2.3), and noting that A^f is independent of x.

Third, the drug consumption rate in the differential volume element dV_c^f may be approximated by a linear reaction having $\beta_d^f > 0$ as an effective first-order consumption rate coefficient. We can write:

$$\begin{pmatrix}\text{drug consumption}\\ \text{rate in element}\end{pmatrix} = -\beta_d^f c_d^f A^f dx \tag{3.23}$$

Fourth, if $\dot{c}_d^f = d\dot{m}_d^f / dV_c^f$ is the mass of substance produced by a chemical reaction per unit time and per unit volume of fluid phase, we have:

$$\begin{pmatrix}\text{drug mass rate produced by chemical}\\ \text{reaction into the elemental volume}\end{pmatrix} = \dot{c}_d^f A^f dx \tag{3.24}$$

Fifth, account must be taken of local mass transfer between solid and fluid phases whose exchange surface into the elemental volume is $P_w dx$, with P_w wetted perimeter. We can write:

$$\begin{pmatrix}\text{mass transfer rate of}\\ \text{drug with solid-phase}\end{pmatrix} = \hbar P_w \left(c_d^s - c_d^f\right) dx \tag{3.25}$$

where $\hbar$ is the solid-fluid local mass transfer coefficient.

Sixth, the mass content of the volume element dV_c^f in terms of drug is $c_d^f A^f dx$. Then, the rate of increase of this mass content is obtained by taking its partial derivative with respect to time, that is, $[\partial(c_d^f A^f)/\partial t]dx$. Therefore, we can write:

$$\begin{pmatrix}\text{rate of increase of drug}\\ \text{mass in element}\end{pmatrix} = A^f \frac{\partial c_d^f}{\partial t} dx \tag{3.26}$$

noting that A^f is also independent of t.

Finally, Eqs. (3.21)–(3.26) are introduced into Eq. (3.20) expressing the conservation of drug in the fluid phase. By some algebra, the fluid phase concentration equation satisfied by the intrinsic volume-averaged concentrations of drug $c_d^f = \left\langle c_d^f \right\rangle^f$, and $c_d^s = \left\langle c_d^s \right\rangle^s$, defined by Eqs. (3.3a) and (3.4a), respectively, is found to be:

$$\underbrace{\varepsilon_k \frac{\partial c_d^f}{\partial t}}_{\text{mass storage}} = \underbrace{\varepsilon_k D_d^f \frac{\partial^2 c_d^f}{\partial x^2}}_{\text{diffusive term}} - \underbrace{\frac{\partial\left(f u c_d^f\right)}{\partial x}}_{\text{advective term}} - \underbrace{\varepsilon_k \beta_d^f c_d^f}_{\text{reaction term}} + \underbrace{\frac{\varepsilon_k \hbar}{r_h}\left(c_d^s - c_d^f\right)}_{\text{local mass transfer}} + \underbrace{\varepsilon_k \dot{c}_d^f}_{\text{mass source}} \tag{3.27a}$$

where r_h is the hydraulic radius (free-flow area A^f/wetted perimeter P_w).

Note, for instance, that $\varepsilon_k \dot{c}_d^f$ is the drug produced by a chemical reaction per unit time and per unit volume of porous medium, while $\dot{c}_d^f$ is the same quantity but per unit volume of fluid phase (i.e., intrinsic). Hence, in Eq. (3.27a), $c_d^f, c_d^s, \beta_d^f, D_d^f, f$ and $\dot{c}_d^f$ are volume-averaged

quantities per unit volume of the fluid phase (intrinsic), whereas u is an average quantity per unit volume of the tissue (porous medium).

The fluid phase concentration equation listed before may also be rewritten in terms of the volume-averaged drug concentrations $\bar{c}_d^f = \langle c_d^f \rangle$ and $\bar{c}_d^s = \langle c_d^s \rangle$ defined by Eqs. (3.3b) and (3.4b), respectively. In such a case, we have:

$$\underbrace{\frac{\partial \bar{c}_d^f}{\partial t}}_{\text{mass storage}} = \underbrace{D_d^f \frac{\partial^2 \bar{c}_d^f}{\partial x^2}}_{\text{diffusive term}} - \underbrace{\frac{1}{\varepsilon_k}\frac{\partial (f u \bar{c}_d^f)}{\partial x}}_{\text{advective term}} - \underbrace{\beta_d^f \bar{c}_d^f}_{\text{reaction term}} + \underbrace{\frac{\hbar}{r_h}\left(\frac{\varepsilon_k}{1-\varepsilon_k}\bar{c}_d^s - \bar{c}_d^f\right)}_{\text{local mass transfer}} + \underbrace{\bar{\dot{c}}_d^f}_{\text{mass source}} \tag{3.27b}$$

where we have used $\langle c_d^f \rangle = \varepsilon_k \langle c_d^f \rangle^f$ and $\langle c_d^s \rangle = (1-\varepsilon_k)\langle c_d^s \rangle^s$ (see Section 3.2.1.1).

In Eq. (3.27b), β_d^f, D_d^f, and f are intrinsic volume-averaged quantities, that is, per unit volume of the fluid phase, whereas $\bar{c}_d^f, \bar{c}_d^s, \bar{\dot{c}}_d^f$ and u are average quantities per unit volume of the tissue (porous medium).

Alternatively, Eq. (3.27) can be obtained by first writing the microscopic drug balance equation for the fluid phase, and then integrating it over V_{rev}. The integrating operation requires the application of well-established theorems such as the transport and averaging theorems ([13] and Section 3.5 of [17]).

3.3.2 Drug Mass Balance in the Solid Phase

In a similar manner, by writing a drug mass balance for a differential volume element in the solid, $dV_c^s = A^s dx$, the conservation equation of substance in the solid matrix phase for the intrinsic volume-averaged drug concentrations $c_d^s = \langle c_d^s \rangle^s$ and $c_d^f = \langle c_d^f \rangle^f$ is:

$$\underbrace{(1-\varepsilon_k)\frac{\partial c_d^s}{\partial t}}_{\text{mass storage}} = \underbrace{(1-\varepsilon_k) D_d^s \frac{\partial^2 c_d^s}{\partial x^2}}_{\text{diffusive term}} - \underbrace{(1-\varepsilon_k)\beta_d^s c_d^s}_{\text{reaction term}} + \underbrace{\frac{\varepsilon_k \hbar}{r_h}\left(c_d^f - c_d^s\right)}_{\text{local mass transfer}} + \underbrace{(1-\varepsilon_k)\dot{c}_d^s}_{\text{mass source}} \tag{3.28a}$$

where the advective term is absent; also, D_d^s is the effective mass diffusivity of the considered substance in the solid phase and β_d^s (positive) is a linear consumption rate coefficient.

The above solid phase concentration equation may also be rewritten in terms of the volume-averaged concentrations of drug $\bar{c}_d^s = \langle c_d^s \rangle$ and $\bar{c}_d^f = \langle c_d^f \rangle$ as follows:

$$\underbrace{\frac{\partial \bar{c}_d^s}{\partial t}}_{\text{mass storage}} = \underbrace{D_d^s \frac{\partial^2 \bar{c}_d^s}{\partial x^2}}_{\text{diffusive term}} - \underbrace{\beta_d^s \bar{c}_d^s}_{\text{reaction term}} + \underbrace{\frac{\hbar}{r_h}\left(\bar{c}_d^f - \frac{\varepsilon_k}{1-\varepsilon_k}\bar{c}_d^s\right)}_{\text{local mass transfer}} + \underbrace{\bar{\dot{c}}_d^s}_{\text{mass source}} \tag{3.28b}$$

where we have used $\langle c_d^s \rangle = (1-\varepsilon_k)\langle c_d^s \rangle^s$ and $\langle c_d^f \rangle = \varepsilon_k \langle c_d^f \rangle^f$ (see Section 3.2.2).

For complete solubility of the drug in the fluid, we have $\varepsilon_k = \varepsilon$ in both Eqs. (3.28).

3.3.3 Governing Equations

Eqs. (3.5), (3.9), (3.27a) and (3.28a) are the governing equations for transient, one-dimensional flow of a fluid through a porous medium, where the fluid that saturates the porous structure is a mixture of two chemical species; for example, drug (solute) and plasma (solvent). The EOS of the fluid needs to be known, as well as the initial and boundary conditions for the unknown variables, namely c_d^f, c_d^s, u and p.

If the temperature of the fluid mixture T^f appearing in EOS is unknown, we also need the conservation-of-energy equation in the fluid phase, which is in turn related to the solid phase energy equation of the porous medium having T^s as unknown (see Subsection 15.2.3 of Ref. [16]). However, for the purposes of this chapter, the mass transfer process will be considered isothermal, and hence the energy balance equations do not play any role.

It is noteworthy to point out that the four partial differential equations (3.5), (3.9), (3.27a) and (3.28a) that govern the conservation of momentum and the conservation of fluid mass and of drug mass are not coupled. This approximation is only valid for dilute systems which, as pointed out in section 3.3.1, are of interest here. First, we can derive the velocity u and pressure p fields by solving the 1-D flow problem described by momentum and continuity equations. Concerning this, we recall that for an incompressible, isothermal fluid, the Darcy velocity u is simply given by Eq. (3.10). Then, once the fluid velocity u appearing in Eq. (3.27a) is known, we can solve the two coupled partial differential Eqs. (3.27a) and (3.28a) expressing the LMNE [13]. This solution will be discussed in the next section where, as we have mixtures of only two components, for simplicity the subscript d will be done away with.

3.4 ANALYTICAL SOLUTIONS FOR LOCAL MASS NON-EQUILIBRIUM

The mathematical difficulties of analytically solving the two coupled partial equations, one for the fluid and the other for the porous material (solid), seem to be insuperable. However, for some special cases, analytical solutions are available in the literature. They come from the theory of heat transfer and will now be briefly revisited and discussed.

Before proceeding to describe them, we note that all the classical special cases (due to Nusselt, Schumann and Anzelius) neglect the diffusive and reaction terms as well as the heat (here, mass) sources or sinks. In addition, as depicted in Fig. 3.8, the porous medium is considered as semi-infinite ($x \geq 0$), the fluid velocity (here, solute velocity fu) uniform and constant, and the boundary and initial conditions for mass transfer are:

$$c^f(x=0,t) = C_{x0}^f \tag{3.29a}$$

$$c^s(x,t=0) = F^s(x) \tag{3.29b}$$

Hence, the boundary condition at $x = 0$ is known only for the drug concentration in the fluid phase. In fact, that in the solid phase cannot be assigned since it comes out as a consequence of the local transfer of drug mass between the two phases, as shown in the next subsections. Similarly, the initial condition $t = 0$ is given only for the drug concentration in the solid phase.

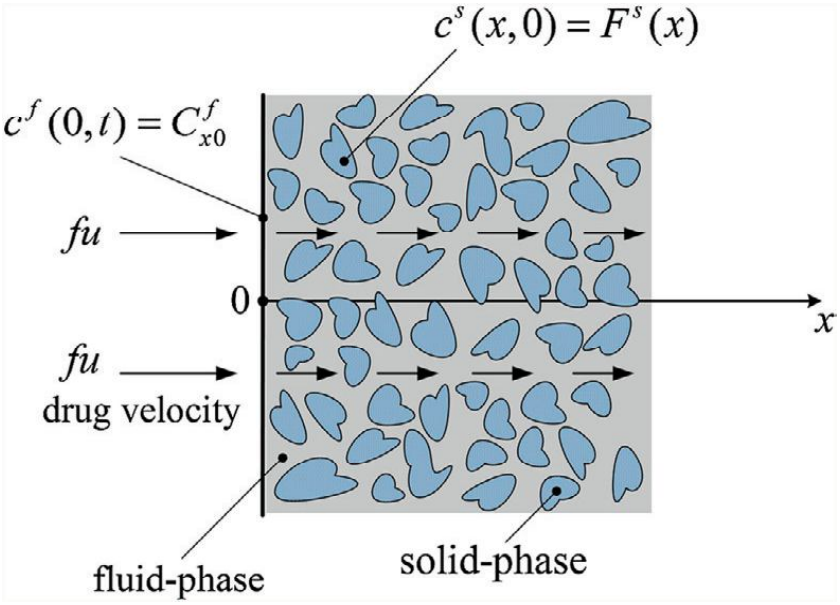

FIGURE 3.8 Schematic of a one-dimensional semi-infinite porous medium.

The one for the fluid phase derives from the interaction with the other phase, as will be shown afterwards.

3.4.1 Nusselt's Solution

Nusselt considered the problem as part of a heat regenerator theory (see Subsection 35–6b of Ref. [18]). For our purposes, with concentration in place of temperature and mass transfer instead of heat transfer, by using the simplifying assumptions stated before, Eqs. (3.27a) and (3.28a) reduce, respectively, to:

$$-r_h \frac{1}{\varepsilon_k} fu \frac{\partial c^f}{\partial x} = \hbar(c^f - c^s) \quad (x > 0; t \geq 0) \tag{3.30a}$$

$$r_h \frac{1-\varepsilon_k}{\varepsilon_k} \frac{\partial c^s}{\partial t} = \hbar(c^f - c^s) \quad (x \geq 0; t > 0) \tag{3.30b}$$

where the drug storage in the fluid phase is neglected.

In Nusselt's former treatment, in fact, the heat storage in the fluid was neglected, which can be done only when the u velocity is very large. However, Nusselt made the general assumption that the solid temperature (here concentration) is an arbitrary function of x at $t = 0$, as shown by Eq. (3.29b).

Equation (3.30a) is not valid at $x = 0$, where the boundary condition Eq. (3.29a) applies, but is valid at the initial time $t = 0$ as the time partial derivative, $\partial/\partial t$, is absent in the

fluid phase equation. For $t = 0$, it reduces to a nonhomogeneous, ordinary, first-order differential equation with constant coefficients, whose solution is:

$$c^f(x,0) = \left[C^f_{x0} + \frac{\hbar}{r_h}\frac{\varepsilon_k}{fu}\int_{\theta=0}^{x} F^s(\theta)\exp\left(\frac{\hbar}{r_h}\frac{\varepsilon_k}{fu}\theta\right)d\theta\right]\exp\left(-\frac{\hbar}{r_h}\frac{\varepsilon_k}{fu}x\right) \tag{3.31a}$$

where the constant of integration has been determined by using Eq. (3.29a).

Equation (3.31a) is to be considered as a second initial condition for $t = 0$, the first being Eq. (3.29b). For the special case of $F^s(x) = C^s_{t0}$ (i.e., uniform), Eq. (3.31a) reduces to:

$$c^f(x,0) = C^s_{t0} + \left(C^f_{x0} - C^s_{t0}\right)\exp\left(-\frac{\hbar}{r_h}\frac{\varepsilon_k}{fu}x\right) = C^f_{x0} + \left(C^s_{t0} - C^f_{x0}\right)\left[1 - \exp\left(-\frac{\hbar}{r_h}\frac{\varepsilon_k}{fu}x\right)\right] \tag{3.31b}$$

Similarly, Eq. (3.30b) is not valid at $t = 0$, where the initial condition Eq. (3.29b) applies, but is valid at the boundary condition $x = 0$ as the space partial derivative, $\partial/\partial x$, is absent in the solid phase equation. For $x = 0$, it becomes a nonhomogeneous, ordinary, first-order differential equation with constant coefficients. Its solution is:

$$c^s(0,t) = C^f_{x0} + \left[F^s(0) - C^f_{x0}\right]\exp\left(-\frac{\hbar}{r_h}\frac{\varepsilon_k}{1-\varepsilon_k}t\right) \tag{3.32a}$$

where the constant of integration has been determined by using Eq. (3.29b).

Equation (3.32a) can be considered as a second boundary condition for $x = 0$, the first being expressed by Eq. (3.29a). For the special case of $F^s(x) = C^s_{t0}$, Eq. (3.32a) becomes:

$$c^s(0,t) = C^f_{x0} + \left(C^s_{t0} - C^f_{x0}\right)\exp\left(-\frac{\hbar}{r_h}\frac{\varepsilon_k}{1-\varepsilon_k}t\right) \tag{3.32b}$$

The solution for the drug concentration in the fluid phase is given in an integral form as (see Eq. (35–52) on p. 277 of Ref. [18]):

$$\begin{aligned} c^f(x,t) = \exp\left[-\frac{\hbar\varepsilon_k}{r_h}\left(\frac{x}{fu} + \frac{t}{1-\varepsilon_k}\right)\right]\cdot\Bigg\{ & C^f_{x0}J_0\left(2i\frac{\hbar\varepsilon_k}{r_h}\sqrt{\frac{xt}{(1-\varepsilon_k)fu}}\right) \\ & + \frac{\hbar\varepsilon_k}{r_h fu}\int_{\theta=0}^{x}\exp\left(\frac{\hbar\varepsilon_k\theta}{r_h fu}\right)F^s(\theta)J_0\left[2i\frac{\hbar\varepsilon_k}{r_h}\sqrt{\frac{t(x-\theta)}{(1-\varepsilon_k)fu}}\right]d\theta \\ & + C^f_{x0}\frac{\hbar}{r_h}\frac{\varepsilon_k}{1-\varepsilon_k}\int_{\theta=0}^{t}\exp\left(\frac{\hbar}{r_h}\frac{\varepsilon_k\theta}{1-\varepsilon_k}\right)J_0\left[2i\frac{\hbar\varepsilon_k}{r_h}\sqrt{\frac{x(t-\theta)}{(1-\varepsilon_k)fu}}\right]d\theta\Bigg\} \end{aligned} \tag{3.33a}$$

where $J_0(z)$ is the Bessel function of the first kind of zero order as in Chap. 9 of Ref. [19], which becomes real for an imaginary argument. In detail, $J_0(0) = 1$ and $J_0(iz) = I_0(z)$, where $I_0(z)$ is the modified Bessel function of the first kind of zero order.

The drug concentration in the solid phase can be derived either by substituting c^f given by Eq. (3.33a) in Eq. (3.30a), after differentiation, or in Eq. (3.30b), after integration. Choosing the former yields:

$$c^s(x,t) = \exp\left(-\frac{\hbar}{r_h}\frac{\varepsilon_k t}{1-\varepsilon_k}\right)F^s(x) - \exp\left[-\frac{\hbar\varepsilon_k}{r_h}\left(\frac{x}{fu}+\frac{t}{1-\varepsilon_k}\right)\right]$$
$$\cdot\left\{C^f_{x0}\sqrt{\frac{fu}{1-\varepsilon_k}\frac{t}{x}}iJ_1\left(2i\frac{\hbar\varepsilon_k}{r_h}\sqrt{\frac{xt}{(1-\varepsilon_k)fu}}\right)\right.$$
$$+\frac{\hbar\varepsilon_k}{r_h}\int_{\theta=0}^{x}\exp\left(\frac{\hbar\varepsilon_k\theta}{r_h fu}\right)F^s(\theta)\sqrt{\frac{1}{(1-\varepsilon_k)fu}\frac{t}{(x-\theta)}}iJ_1\left[2i\frac{\hbar\varepsilon_k}{r_h}\sqrt{\frac{t(x-\theta)}{(1-\varepsilon_k)fu}}\right]d\theta$$
$$\left.+C^f_{x0}\frac{\hbar\varepsilon_k}{r_h}\frac{fu}{1-\varepsilon_k}\int_{\theta=0}^{t}\exp\left(\frac{\hbar}{r_h}\frac{\varepsilon_k\theta}{1-\varepsilon_k}\right)\sqrt{\frac{1}{(1-\varepsilon_k)fu}\frac{(t-\theta)}{x}}iJ_1\left[2i\frac{\hbar\varepsilon_k}{r_h}\sqrt{\frac{x(t-\theta)}{(1-\varepsilon_k)fu}}\right]d\theta\right\} \tag{3.33b}$$

where $J_1(z)$ is the Bessel function of the first kind of first order [19] which, when multiplied by the imaginary unit i, becomes real for an imaginary argument. In detail, $iJ_1(iz) = -I_1(z)$, where $I_1(z)$ is the modified Bessel function of the first kind of first order.

The solution development in the fluid phase is clearly described in [20]. Nusselt did not solve the integrals appearing in the two equations listed before. It can be proved that, for $t = 0$, the former reduces to Eq. (3.31a) and, hence, to Eq. (3.31b) when $F^s(x) = C^s_{t0}$. By some algebra, for $x = 0$, the latter reduces to Eq. (3.32a) and, hence, to Eq. (3.32b) when $F^s(x) = C^s_{t0}$.

For the special case of $F^s(x) = C^s_{t0}$, the governing Eqs. (3.29)–(3.30) may conveniently be rewritten in a dimensionless form by using the following variables:

$$\tilde{x} = \frac{\hbar}{r_h}\frac{\varepsilon_k}{fu}x \quad \tilde{t} = \frac{\hbar}{r_h}\frac{\varepsilon_k}{1-\varepsilon_k}t \quad \tilde{c} = \frac{c - C^f_{x0}}{C^s_{t0} - C^f_{x0}} \tag{3.34}$$

where the $r_h/\hbar$ ratio (having units of s) can be considered as a time constant characterizing the local transfer of drug between the solid and fluid phases.

In dimensionless form, the defining equations become:

$$-\frac{\partial\tilde{c}^f}{\partial\tilde{x}} = (\tilde{c}^f - \tilde{c}^s) \quad (\tilde{x} > 0; \tilde{t} \geq 0) \tag{3.35a}$$

$$\frac{\partial\tilde{c}^s}{\partial\tilde{t}} = (\tilde{c}^f - \tilde{c}^s) \quad (\tilde{x} \geq 0; \tilde{t} > 0) \tag{3.35b}$$

$$\tilde{c}^f(\tilde{x} = 0, \tilde{t}) = 0 \tag{3.35c}$$

$$\tilde{c}^s(\tilde{x}, \tilde{t} = 0) = 1 \tag{3.35d}$$

whose concentration solutions may be derived from Eqs. (3.33a) and (3.33b) as, respectively:

$$\tilde{c}^f(\tilde{x},\tilde{t}) = \exp[-(\tilde{x}+\tilde{t})] \cdot \int_{\tilde{\theta}=0}^{\tilde{x}} \exp(\tilde{\theta}) I_0\left[2\sqrt{\tilde{t}(\tilde{x}-\tilde{\theta})}\right] d\tilde{\theta} \tag{3.36a}$$

$$\tilde{c}^s(\tilde{x},\tilde{t}) = \exp(-\tilde{t}) + \exp\left[-(\tilde{x}+\tilde{t})\right] \cdot \int_{\tilde{\theta}=0}^{\tilde{x}} \exp(\tilde{\theta}) \sqrt{\frac{\tilde{t}}{\tilde{x}-\tilde{\theta}}} I_1\left[2\sqrt{\tilde{t}(\tilde{x}-\tilde{\theta})}\right] d\tilde{\theta} \tag{3.36b}$$

It should be noted that the evaluation of the analytical solutions of Eq. (3.36) requires numerical integration. This was done using an adaptive Gauss-Kronod quadrature scheme in Matlab ambient. Plots of the solutions are given in Fig. 3.9, for which the dimensionless

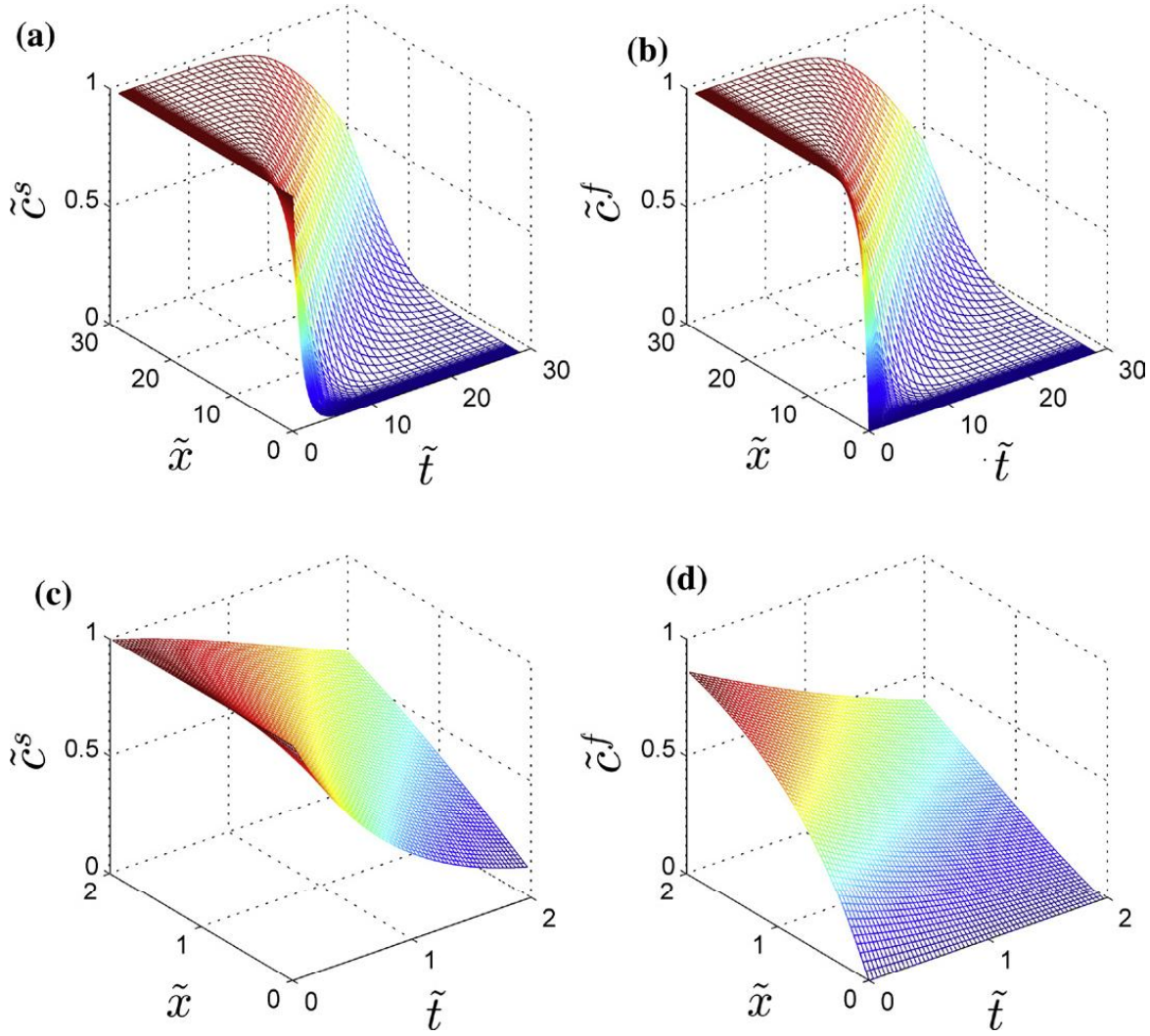

FIGURE 3.9 Dimensionless concentration profiles as function of space and time: (a) solid phase; (b) fluid phase; (c) solid phase for small values of locations and times, and (d) fluid phase for small values of locations and times.

solid phase concentration, cases (a) and (c), rapidly diminishes at small values of $\tilde{x}$ when the time increases, while the further locations take much longer to feel the influence of the fluid within the porous media. In particular, at the boundary surface $\tilde{x} = 0$, we have an exponential decay as indicated by Eq. (3.31b) that, in dimensionless form, becomes $\tilde{c}^s(0,\tilde{t}) = \exp(-\tilde{t})$. The non-dimensional fluid phase concentration, cases (b) and (d), has zero value at the boundary $\tilde{x} = 0$, and then increases with $\tilde{x}$ as drug is released from the solid phase. For $\tilde{t} = 0$, it increases exponentially as given by Eq. (3.31b) that, in dimensionless form, becomes $\tilde{c}^f(\tilde{x},0) = 1 - \exp(-\tilde{x})$. It is interesting to note that both solutions are similar for large values of $\tilde{x}$ and $\tilde{t}$, cases a) and b), which makes sense physically. The LMNE is evident only for small values of $\tilde{x}$ and $\tilde{t}$, cases (c) and (d).

3.4.2 Schumann's Solution

It is worth mentioning that Schumann considered the problem as part of a porous medium theory (see Subsection 35–6c of Ref. [18,21]). His goal was in fact to quantify the heating up of a porous prism through which a liquid was flowing. For the purposes that are of interest here, concentration is put in place of temperature and mass transfer instead of heat transfer, so by using the simplifying assumptions stated in Section 3.4, Eqs. (3.27a) and (3.28a) reduce, respectively, to:

$$\varepsilon_k \frac{\partial c^f}{\partial t} + fu \frac{\partial c^f}{\partial x} = -\frac{\hbar \varepsilon_k}{r_h}(c^f - c^s) \quad (x > 0; t > 0) \tag{3.37a}$$

$$r_h \frac{1-\varepsilon_k}{\varepsilon_k} \frac{\partial c^s}{\partial t} = \hbar(c^f - c^s) \quad (x \geq 0; t > 0) \tag{3.37b}$$

where the term $\partial/\partial t$ in the fluid phase (indicating drug storage) is now taken into account.

According to Schumann's former treatment where the solid temperature was assumed to be uniform at $t = 0$, the initial condition Eq. (3.29b) has to be replaced by:

$$c^s(x, t = 0) = C^s_{t0} \tag{3.38}$$

Note that Eq. (3.37b) is also valid at the boundary condition $x = 0$ in accordance with the absence of the space partial derivative, $\partial/\partial x$. For $x = 0$, it reduces to a nonhomogeneous, ordinary differential equation of the first order with constant coefficients. Its solution is given by Eq. (3.32b), which can be considered as a second boundary condition for $x = 0$, the first being Eq. (3.29a).

On the contrary, Eq. (3.37a) does not apply at the initial time $t = 0$ consistently to the presence of the time partial derivative, $\partial/\partial t$. Hence, an initial condition for $c^f(x,t)$ has to be assigned as:

$$c^f(x, t = 0) = C^s_{t0} \tag{3.39}$$

Equations (3.38) and (3.39) state that there exists a LME between the two phases at $t = 0$. As the diffusive term is absent in both the drug balance equations, namely Eqs. (3.37a) and

(3.37b), the above equilibrium at $t = 0$ keeps up to $t = x/(fu)$. The quantity $x/(fu)$ is the time that it takes for a drug particle in the fluid phase flowing through the semi-infinite porous structure ($x \geq 0$) of Fig. 3.8 to reach the location x of interest with a velocity of fu.

The solution for the drug concentration in both phases is given in an integral form as (see Eqs. (35–65) and (35–66) on p. 280 of Ref. [18]):

$$\begin{aligned}\frac{c^f(x,t) - C^s_{t0}}{C^f_{x0} - C^s_{t0}} &= \exp\left(-\frac{\hbar}{r_h}\frac{\varepsilon_k}{fu}x\right) \\ &\cdot \left\{\exp\left[-\frac{\hbar}{r_h}\frac{\varepsilon_k}{1-\varepsilon_k}\left(t - \frac{x}{fu}\right)\right] J_0\left[2i\frac{\hbar\varepsilon_k}{r_h}\sqrt{\frac{x}{fu}\frac{1}{1-\varepsilon_k}\left(t - \frac{x}{fu}\right)}\right]\right. \\ &\left. + \frac{\hbar}{r_h}\frac{\varepsilon_k}{1-\varepsilon_k}\int_{\theta=0}^{t-\frac{x}{fu}} \exp\left(-\frac{\hbar}{r_h}\frac{\varepsilon_k}{1-\varepsilon_k}\theta\right) J_0\left(2i\frac{\hbar\varepsilon_k}{r_h}\sqrt{\frac{x}{fu}\frac{\theta}{1-\varepsilon_k}}\right) d\theta\right\}\end{aligned} \tag{3.40a}$$

$$\begin{aligned}\frac{c^s(x,t) - C^s_{t0}}{C^f_{x0} - C^s_{t0}} &= \frac{\hbar}{r_h}\frac{\varepsilon_k}{1-\varepsilon_k}\exp\left(-\frac{\hbar}{r_h}\frac{\varepsilon_k}{fu}x\right) \\ &\cdot \int_{\theta=0}^{t-\frac{x}{fu}} \exp\left(-\frac{\hbar}{r_h}\frac{\varepsilon_k}{1-\varepsilon_k}\theta\right) J_0\left(2i\frac{\hbar\varepsilon_k}{r_h}\sqrt{\frac{x}{fu}\frac{\theta}{1-\varepsilon_k}}\right) d\theta\end{aligned} \tag{3.40b}$$

For a given location x, the above equations apply only for $t \geq x/(fu)$. For $0 \leq t < x/(fu)$, we have $c^f(x,t) = c^s(x,t) = C^s_{t0}$. For $t = x/(fu)$, they reduce, respectively, to:

$$\frac{c^f(x) - C^s_{t0}}{C^f_{x0} - C^s_{t0}} = \exp\left(-\frac{\hbar}{r_h}\frac{\varepsilon_k}{fu}x\right) \quad \frac{c^s(x) - C^s_{t0}}{C^f_{x0} - C^s_{t0}} = 0 \tag{3.41}$$

For a given time t, Eqs. (3.40a) and (3.40b) apply only for $0 \leq x \leq (fu)t$. For $x = (fu)t$, they reduce, respectively, to:

$$\frac{c^f(t) - C^s_{t0}}{C^f_{x0} - C^s_{t0}} = \exp\left(-\frac{\hbar\varepsilon_k}{r_h}t\right) \quad \frac{c^s(t) - C^s_{t0}}{C^f_{x0} - C^s_{t0}} = 0 \tag{3.42}$$

For $x > (fu)t$, we have a LME, i.e., $c^f(x,t) = c^s(x,t) = C^s_{t0}$, where $(fu)t$ is the distance traveled (from the boundary surface $x = 0$) by a drug particle flowing in the fluid phase of the porous medium with a fu velocity during the time t of interest.

After some lengthy algebraic manipulations, Schumann was able to solve the integrals of Eqs. (3.40a) and (3.40b), arriving at two infinite series which he solved explicitly (more details can be found in Subsection 35–6.c of Ref. [18,21]).

Note that the drug concentration in the solid phase can alternatively be derived by substituting c^f given by Eq. (3.40a) in Eq. (3.37a), and performing two differentiations, or in Eq. (3.37b), and performing one integration. In addition, combining Eqs. (3.40a) and (3.40b) yields the following drug concentration difference between the two phases:

$$\frac{c^s(x,t)-c^f(x,t)}{C^s_{t0}-C^f_{x0}} = I_0\left[2\frac{\hbar\varepsilon_k}{r_h}\sqrt{\frac{x}{fu}\frac{1}{1-\varepsilon_k}\left(t-\frac{x}{fu}\right)}\right]\cdot\exp\left[-\frac{\hbar}{r_h}\frac{\varepsilon_k}{1-\varepsilon_k}\left(t-\frac{x}{fu}\right)\right] \quad (t\geq x/(fu)) \tag{3.43}$$

where we have used $J_0(iz)=I_0(z)$.

By using the dimensionless variables as defined by Eq. (3.34), we have that Eq. (3.43) becomes:

$$\tilde{c}^s(\tilde{x},\tilde{t})-\tilde{c}^f(\tilde{x},\tilde{t}) = I_0\left[2\sqrt{\tilde{x}\left(\tilde{t}-\frac{\tilde{x}}{1-\varepsilon_k}\right)}\right]\cdot\exp\left[-\left(\tilde{t}-\frac{\tilde{x}}{1-\varepsilon_k}\right)\right] \quad (\tilde{t}\geq\tilde{x}/(1-\varepsilon_k)) \tag{3.44}$$

Hence, the above dimensionless drug concentration difference depends not only on the non-dimensional space and time but also on the available volume fraction ε_k.

3.4.3 Anzelius's Solution

Anzelius's work concerned the heating of a fluid flowing through a hot porous matrix. The partial differential equations he used are exactly the same as the ones used by Schumann; that is, Eqs. (3.37a) and (3.37b), with boundary and initial conditions given by Eqs. (3.29a), (3.38) and (3.39), respectively. The solution is given in an integral form as (see Eqs. (16) and (17) on p. 394 of Ref. [22]):

$$\begin{aligned}\frac{c^f(x,t)-C^s_{t0}}{C^f_{x0}-C^s_{t0}} =& \exp\left(-\frac{\hbar}{r_h}\frac{\varepsilon_k}{fu}x\right)\\ &\cdot\left\{1+\frac{\hbar\varepsilon_k}{r_h}\sqrt{\frac{1}{1-\varepsilon_k}\frac{x}{fu}}\int_{\theta=0}^{t-\frac{x}{fu}}\exp\left(-\frac{\hbar}{r_h}\frac{\varepsilon_k}{1-\varepsilon_k}\theta\right)\frac{1}{\sqrt{\theta}}I_1\left(2\frac{\hbar\varepsilon_k}{r_h}\sqrt{\frac{1}{1-\varepsilon_k}\frac{x}{fu}\theta}\right)d\theta\right\}\end{aligned} \tag{3.45a}$$

$$\begin{aligned}\frac{c^s(x,t)-C^s_{t0}}{C^f_{x0}-C^s_{t0}} =& \frac{\hbar}{r_h}\frac{\varepsilon_k}{1-\varepsilon_k}\exp\left(-\frac{\hbar}{r_h}\frac{\varepsilon_k}{fu}x\right)\\ &\cdot\int_{\theta=0}^{t-\frac{x}{fu}}\exp\left(-\frac{\hbar}{r_h}\frac{\varepsilon_k}{1-\varepsilon_k}\theta\right)I_0\left(2\frac{\hbar\varepsilon_k}{r_h}\sqrt{\frac{x}{fu}\frac{\theta}{1-\varepsilon_k}}\right)d\theta\end{aligned} \tag{3.45b}$$

For a given location x, the above equations apply only for $t \geq x/(fu)$. For a given time t, they apply only for $x \leq (fu)t$. Also, note that Eq. (3.45a) derived by Anzelius is exactly the same as Eq. (3.40a) obtained by Schumann. In fact, by using the relation $I_0(z) = J_0(iz)$, Eq. (3.40a) becomes:

$$\frac{c^f(x,t) - C^s_{t0}}{C^f_{x0} - C^s_{t0}} = \left\{ \exp\left[-\frac{\hbar}{r_h} \frac{\varepsilon_k}{1-\varepsilon_k} \left(t - \frac{x}{fu} \right) \right] \cdot I_0 \left[2 \frac{\hbar \varepsilon_k}{r_h} \sqrt{ \frac{x}{fu} \frac{1}{1-\varepsilon_k} \left(t - \frac{x}{fu} \right) } \right] \right.$$
$$\left. + \frac{\hbar}{r_h} \frac{\varepsilon_k}{1-\varepsilon_k} \int_{\theta=0}^{t-\frac{x}{fu}} \exp\left(-\frac{\hbar}{r_h} \frac{\varepsilon_k}{1-\varepsilon_k} \theta \right) I_0 \left(2 \frac{\hbar \varepsilon_k}{r_h} \sqrt{ \frac{x}{fu} \frac{\theta}{1-\varepsilon_k} } \right) d\theta \right\}$$
$$\cdot \exp\left(-\frac{\hbar}{r_h} \frac{\varepsilon_k}{fu} x \right) \tag{3.46}$$

By integrating the integral on the RHS of the above equation by parts, and recalling that $dI_0(z)/dz = I_1(z)$ (see p. 376, Eq. (9.6.27) of Ref. [19]), we obtain exactly Eq. (3.45a). Similarly, as $I_0(z) = J_0(iz)$, Eq. (3.45b) is exactly the same as Eq. (3.40b).

Then, by using the dimensionless variables as defined by Eq. (3.34), Eqs. (3.45a) and (3.45b) become, respectively:

$$\tilde{c}^f(\tilde{x},\tilde{t}) = 1 - \exp(-\tilde{x}) \cdot \left[1 + \sqrt{\tilde{x}} \int_{\tilde{\theta}=0}^{\tilde{t}-\frac{\tilde{x}}{1-\varepsilon_k}} \exp(-\tilde{\theta}) \frac{1}{\sqrt{\tilde{\theta}}} I_1\left(2\sqrt{\tilde{x}\tilde{\theta}} \right) d\tilde{\theta} \right] \quad (\tilde{t} \geq \tilde{x}/(1-\varepsilon_k)) \tag{3.47a}$$

$$\tilde{c}^s(\tilde{x},\tilde{t}) = 1 - \exp(-\tilde{x}) \cdot \int_{\tilde{\theta}=0}^{\tilde{t}-\frac{\tilde{x}}{1-\varepsilon_k}} \exp(-\tilde{\theta}) \cdot I_0\left(2\sqrt{\tilde{x}\tilde{\theta}} \right) d\tilde{\theta} \quad (\tilde{t} \geq \tilde{x}/(1-\varepsilon_k)) \tag{3.47b}$$

3.4.4 Recent Solutions

Recent analytical solutions and physical analysis for the Schumann model (based on a perturbation technique) were obtained by Kuznetsov in Refs. [23–25]. In particular, these papers demonstrated that the wave describing a temperature difference between the fluid and solid phases (in terms of the present paper, a concentration difference) forms a wave that is localized in space and propagates in the direction of the flow. As the wave propagates, it spreads out and its amplitude decreases. This new physical behavior of the temperature (or concentration) difference was first shown in the above papers.

In addition, following *Tzou*'s approach [26], *Haji-Sheikh et al*. were able to obtain analytical solutions using Green's functions for both fluid and solid phases of a porous medium subject to rapid transient heating (or cooling) [27,28]. In such a case, in fact, the local thermal equilibrium (LTE) hypothesis is usually not valid. A criterion for LTE based on the magnitude of the Sparrow number and on the rate of change of the heat input was developed and proposed. Its extension to LME is subject of future research.

3.5 ANALYTICAL SOLUTIONS FOR LOCAL MASS EQUILIBRIUM

In many cases, it is acceptable to assume a LME so that $c^f = c^s = c$. Then, assuming that the drug velocity fu in the fluid phase is uniform and constant, summing up Eqs. (3.27a) and (3.28a) yields:

$$\frac{\partial c}{\partial t} = \overline{D}\frac{\partial^2 c}{\partial x^2} - (fu)\frac{\partial c}{\partial x} - \bar{\beta}c + \bar{\dot{c}} \tag{3.48}$$

where $\overline{D}, \overline{\beta}$ and $\bar{\dot{c}}$ are, respectively, the overall effective diffusivity, the overall consumption rate coefficient and the overall mass production rate, all of them per unit volume of porous medium. They may be taken as:

$$\overline{D} = (1-\varepsilon_k)D^s + \varepsilon_k D^f \tag{3.49a}$$

$$\bar{\beta} = (1-\varepsilon_k)\beta^s + \varepsilon_k \beta^f \tag{3.49b}$$

$$\bar{\dot{c}} = (1-\varepsilon_k)\dot{c}^s + \varepsilon_k \dot{c}^f \tag{3.49c}$$

Hence, by assuming that at any point in the solid-fluid porous matrix the two concentrations are identical, the analysis can significantly be simplified. In particular, when there is no motion and reaction through the pores of the solid structure, we have pure mass diffusion. This means that the mathematical methods developed for diffusion in solids [22,29,30] apply to porous media saturated with stagnant fluid with no reaction. However, if the convection and reaction terms are present in the LME-based Eq. (3.48), by some appropriate transformations the problem can still be reduced to a pure diffusive one, as shown in the next subsection.

3.5.1 A Worked Example

A finite polymeric matrix of available volume fraction ε_k and thickness l contains drug initially at a uniform concentration C^s_{t0}, as depicted in Fig. 3.10. Plasma at the same drug concentration C^s_{t0} flows through the matrix with velocity $u_p \approx u$ (averaged over r.e.v.), where u is the velocity of the binary mixture of plasma and drug (for dilute systems, $u_p \approx u$). Therefore, the initial conditions for the solid and fluid phases are, respectively:

$$(1-\varepsilon_k)c^s(x, t=0) = (1-\varepsilon_k)C^s_{t0} \quad (0 < x < l) \tag{3.50a}$$

$$\varepsilon_k c^f(x, t=0) = \varepsilon_k C^s_{t0} \quad (0 < x < l) \tag{3.50b}$$

For $t > 0$, the concentration of drug at the plasma inlet $x = 0$ the concentration of drug is kept at C^f_{x0}. At the opposite boundary surface $x = l$ a highly resistive drug barrier allows the plasma to pass while restricting the drug's transport, effectively acting as a no-flux boundary condition. This is depicted in Fig. 3.10. The boundary conditions for the solid and fluid phases at $x = 0$ and $x = l$ are, respectively:

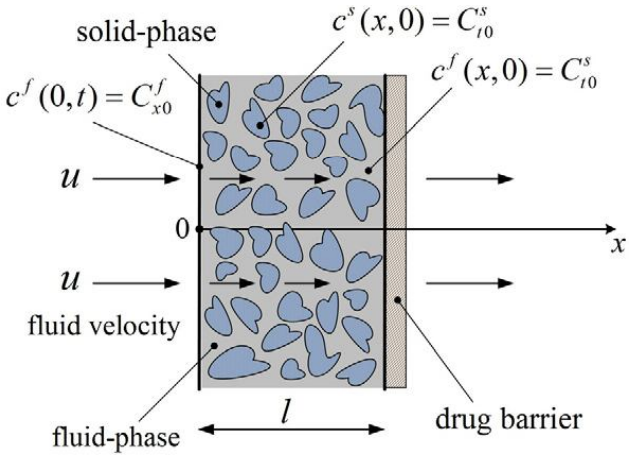

FIGURE 3.10 Schematic of a one-dimensional finite polymeric matrix (porous medium) with a drug barrier at $x = l$.

- $x = 0$

$$\hbar_0(1-\varepsilon_k)\left[C^f_{x0} - c^s(x=0,t)\right] = -D^s(1-\varepsilon_k)\left(\frac{\partial c^s}{\partial x}\right)_{x=0} \quad (t>0) \tag{3.51a}$$

$$\varepsilon_k c^f(x=0,t) = \varepsilon_k C^f_{x0} \quad (t>0) \tag{3.51b}$$

- $x = l$

$$-D^s(1-\varepsilon_k)\left(\frac{\partial c^s}{\partial x}\right)_{x=l} = 0 \quad (t>0) \tag{3.52a}$$

$$-D^f\varepsilon_k\left(\frac{\partial c^f}{\partial x}\right)_{x=l} = 0 \quad (t>0) \tag{3.52b}$$

where $\hbar_0$ is the mass transfer coefficient at $x = 0$.

Equations (3.50) state that there exists a LME between solid and fluid phases at $t = 0$. On the contrary, Eqs. (3.51) say that there exists no mass equilibrium at $x = 0$. However, if we assume that $\hbar_0$ is very large ($\hbar_0 \to \infty$), we have mass equilibrium at $x = 0$ too, and Eq. (3.51a) reduces to:

$$(1-\varepsilon_k)c^s(x=0,t) = (1-\varepsilon_k)C^f_{x0} \quad (t>0) \tag{3.53}$$

Now, for the sake of simplicity, the approximation of LME is made not only at $x = 0$, but at any location x in the solid-fluid porous matrix. Consequently, Eq. (3.48), expressing the conservation of drug in the whole porous medium, holds. When mass generation and reaction terms are absent, it reduces to:

$$\frac{\partial \theta}{\partial t} = \overline{D}\frac{\partial^2 \theta}{\partial x^2} - (fu)\frac{\partial \theta}{\partial x} \quad (0 < x < l; t > 0) \tag{3.54}$$

where the reduced concentration $\theta(x,t) = c(x,t) - C^s_{t0}$ has been used. Looking ahead in the analysis, in fact, it makes the initial concentration zero, hence simplifying the derivation of the solution, as will be shown in the next paragraph.

Also, the boundary and initial conditions collapse into:

$$\theta(0,t) = \theta_0 \quad \left(\frac{\partial c}{\partial x}\right)_{x=l} = 0 \quad (t > 0) \tag{3.55a}$$

$$\theta(x, t = 0) = 0 \quad (0 < x < l) \tag{3.55b}$$

where $\theta_0 = C^f_{x0} - C^s_{t0}$.

Solution

The above defining Eqs. (3.56a)–(3.56c) are transformed using the following relation ([31] and p. 91 of [30]):

$$\theta(x,t) = w(x,t) \cdot \exp\left[\frac{fu}{2\overline{D}}x - \frac{(fu)^2}{4\overline{D}}t\right] \tag{3.56}$$

where $w(x,t)$ is a new dependent variable.

Substituting the above equation in the governing Eqs. (3.54)–(3.55), we obtain:

$$\frac{\partial w}{\partial t} = \overline{D}\frac{\partial^2 w}{\partial x^2} \quad (0 < x < l; t > 0) \tag{3.57a}$$

$$w(0,t) = \theta_0 \exp\left[\frac{(fu)^2}{4\overline{D}}t\right] \quad (t > 0) \tag{3.57b}$$

$$-\overline{D}\left(\frac{\partial w}{\partial x}\right)_{x=l} = \hbar_{le} w(l,t) \quad (t > 0) \tag{3.57c}$$

$$w(x,0) = 0 \quad (0 < x < l) \tag{3.57d}$$

where $\hbar_{le} = fu/2$ is the effective mass transfer coefficient at $x = l$. Also, as in Eq. (3.57c) we have $\overline{D}$ defined by Eq. (3.49a) in place of D^s, the plasma seems to play an active role in this boundary condition (see p. 167 of [32]).

The concentration solution to Eqs. (3.57a)–(3.57d) may be obtained by using Green's function (GF) solution equation (see p. 66 of [30]):

$$w(x,t) = -\overline{D}\theta_0 \int_{\tau=0}^{t} \exp\left[\frac{(fu)^2}{4\overline{D}}\tau\right] \cdot \left[-\frac{\partial}{\partial x'} G_{X13}(x,x',t-\tau)\right]_{x'=0} d\tau \tag{3.58}$$

where the large-cotime form of $G_{X13}(x,x',t-\tau)$ is on p. 590 of Ref. [30]:

$$G_{X13}(x,x',t-\tau) = \frac{2}{l}\sum_{n=1}^{\infty} \frac{\beta_n^2 + Bi_{le}^2}{\beta_n^2 + Bi_{le}^2 + Bi_{le}} \sin\left(\beta_n \frac{x}{l}\right) \sin\left(\beta_n \frac{x'}{l}\right) \exp\left[-\frac{\beta_n^2 \overline{D}}{l^2}(t-\tau)\right] \tag{3.59}$$

(The subscript X indicates mass diffusion along the x-axis; 1 and 3 denote the boundary conditions of the 1st and 3rd kind at $x = 0$ and $x = l$, respectively. More details can be found in Chap. 2 of Ref. [30] for the notation system devised by *Beck et al.*).

The β_n is the nth dimensionless eigenvalue of the following eigencondition: $\beta_n \cot \beta_n = -Bi_{le}$, where $Bi_{le} = \hbar_{le} l/\overline{D}$ is the effective Biot number at $x = l$. The β_n eigenvalues may be computed by using explicit approximate equations with six-digit accuracy developed by *Haji-Sheikh and Beck* [33]. Substituting the large-cotime GF (3.59) in Eq. (3.58) and integrating gives:

$$\begin{aligned} w(x,t) = 2\theta_0 \sum_{n=1}^{\infty} &\frac{\beta_n^2 + Bi_{le}^2}{\beta_n^2 + Bi_{le}^2 + Bi_{le}} \frac{\beta_n}{(fPe/2)^2 + \beta_n^2} \sin\left(\beta_n \frac{x}{l}\right) \\ &\cdot \left\{\exp\left[\frac{(fu)^2}{4\overline{D}}t\right] - \exp\left(-\frac{\beta_n^2 \overline{D}}{l^2}t\right)\right\} \end{aligned} \tag{3.60}$$

where $Pe = ul/\overline{D}$ is the Péclet number associated with the fluid.

Once $w(x,t)$ is obtained, the transformation (3.56) can be inverted to find the concentration of drug. Then, we have:

$$\begin{aligned} \theta(x,t) = 2\theta_0 \exp\left(f\frac{Pe}{2}\frac{x}{l}\right) \cdot \sum_{n=1}^{\infty} &\frac{\beta_n^2 + Bi_{le}^2}{\beta_n^2 + Bi_{le}^2 + Bi_{le}} \frac{\beta_n}{(fPe/2)^2 + \beta_n^2} \sin\left(\beta_n \frac{x}{l}\right) \\ - 2\theta_0 \exp\left(f\frac{Pe}{2}\frac{x}{l}\right) \cdot \sum_{n=1}^{\infty} &\frac{\beta_n^2 + Bi_{le}^2}{\beta_n^2 + Bi_{le}^2 + Bi_{le}} \frac{\beta_n}{(fPe/2)^2 + \beta_n^2} \sin\left(\beta_n \frac{x}{l}\right) \\ \cdot \exp\left\{-\left[\left(f\frac{Pe}{2}\right)^2 + \beta_n^2\right]\frac{\bar{D}t}{l^2}\right\} & \end{aligned} \tag{3.61}$$

where the steady state part (first term on the RHS) has an algebraic convergence (very slow).

Using the following algebraic identity (see App. B, p. 267 of Ref. [34]):

$$\begin{aligned} 2\sum_{n=1}^{\infty} &\frac{\beta_n^2 + Bi_{le}^2}{\beta_n^2 + Bi_{le}^2 + Bi_{le}} \frac{\beta_n}{(fPe/2)^2 + \beta_n^2} \sin\left(\beta_n \frac{x}{l}\right) \\ &= \frac{(fPe + 2Bi_{le})e^{-f\frac{Pe}{2}\frac{x}{l}} + (fPe - 2Bi_{le}) \cdot \exp\left[-f\frac{Pe}{2}\left(2 - \frac{x}{l}\right)\right]}{(fPe + 2Bi_{le}) + (fPe - 2Bi_{le}) \cdot \exp\left(-fPe\right)}, \end{aligned} \tag{3.62}$$

and also noting that $Bi_{le} = \hbar_{le} l/\overline{D} = ful/2\overline{D} = fPe/2$, Eq. (3.61) becomes:

$$\theta(x,t) = \theta_0 - 2\theta_0 \exp\left(f\frac{Pe}{2}\frac{x}{l}\right) \cdot \sum_{n=1}^{\infty} \frac{\beta_n}{\beta_n^2 + (fPe/2)^2 + fPe/2} \sin\left(\beta_n \frac{x}{l}\right) \cdot \exp\left\{-\left[\left(f\frac{Pe}{2}\right)^2 + \beta_n^2\right]\frac{\overline{D}t}{l^2}\right\} \tag{3.63}$$

which reduces to the well-known solution given in the literature when $u = 0 (\Rightarrow Pe = 0)$. This is an application of the 'symbolic' intrinsic verification (see Chap. 5 of Ref. [30,35]). In a dimensionless form, we have:

$$\tilde{c}(\tilde{x},\tilde{t}) = 1 - 2\exp\left(f\frac{Pe}{2}\tilde{x}\right) \cdot \sum_{n=1}^{\infty} \frac{\beta_n}{\beta_n^2 + (fPe/2)^2 + fPe/2} \sin\left(\beta_n \tilde{x}\right) \cdot \exp\left\{-\left[\left(f\frac{Pe}{2}\right)^2 + \beta_n^2\right]\tilde{t}\right\} \tag{3.64}$$

where:

$$\tilde{x} = \frac{x}{l} \quad \tilde{t} = \frac{\overline{D}t}{l^2} \quad \tilde{c} = \frac{\theta}{\theta_0} = \frac{c - C_{t0}^s}{C_{x0}^f - C_{t0}^s} \tag{3.65}$$

The plots in Fig. 3.11 depict the evaluation of the solution to the dimensionless solute concentration as a function of dimensionless position and time for different Péclet numbers with a retardation coefficient $f = 0.5$. At very short times, the Péclet number has no noticeable influence on the distribution, and the presence of convective influences at early times is only noticeable for $Pe \sim 10$. At longer times, even minor convective influences are noticeable at locations far from the source.

Next, to quantify the influence of Pe on transient behavior, the dimensionless drug mass per unit area $\tilde{M}$ contained within the domain has been plotted as a function of time for $f = 0.5$, as shown in Fig. 3.12. The dimensionless drug mass may be calculated as:

$$\tilde{M}(\tilde{t}) = \int_{\tilde{x}=0}^{1} \tilde{c}(\tilde{x},\tilde{t}) d\tilde{x} \tag{3.66}$$

where $\tilde{M}$ is defined as:

$$\tilde{M} = \frac{M - C_{t0}^s l}{\theta_0 l} = \frac{M - C_{t0}^s l}{(C_{x0}^f - C_{t0}^s) l} \tag{3.67}$$

At $Pe = 0$, the mass is slowly transported by diffusion. As convective influences increase (with increasing values of Pe), the rate at which the mass is transported also increases. Comparing the times at which the steady state concentration is approached for $Pe = 0$ around and $Pe = 10$ it is evident that even a small convective contribution will greatly speed up the drug transfer.

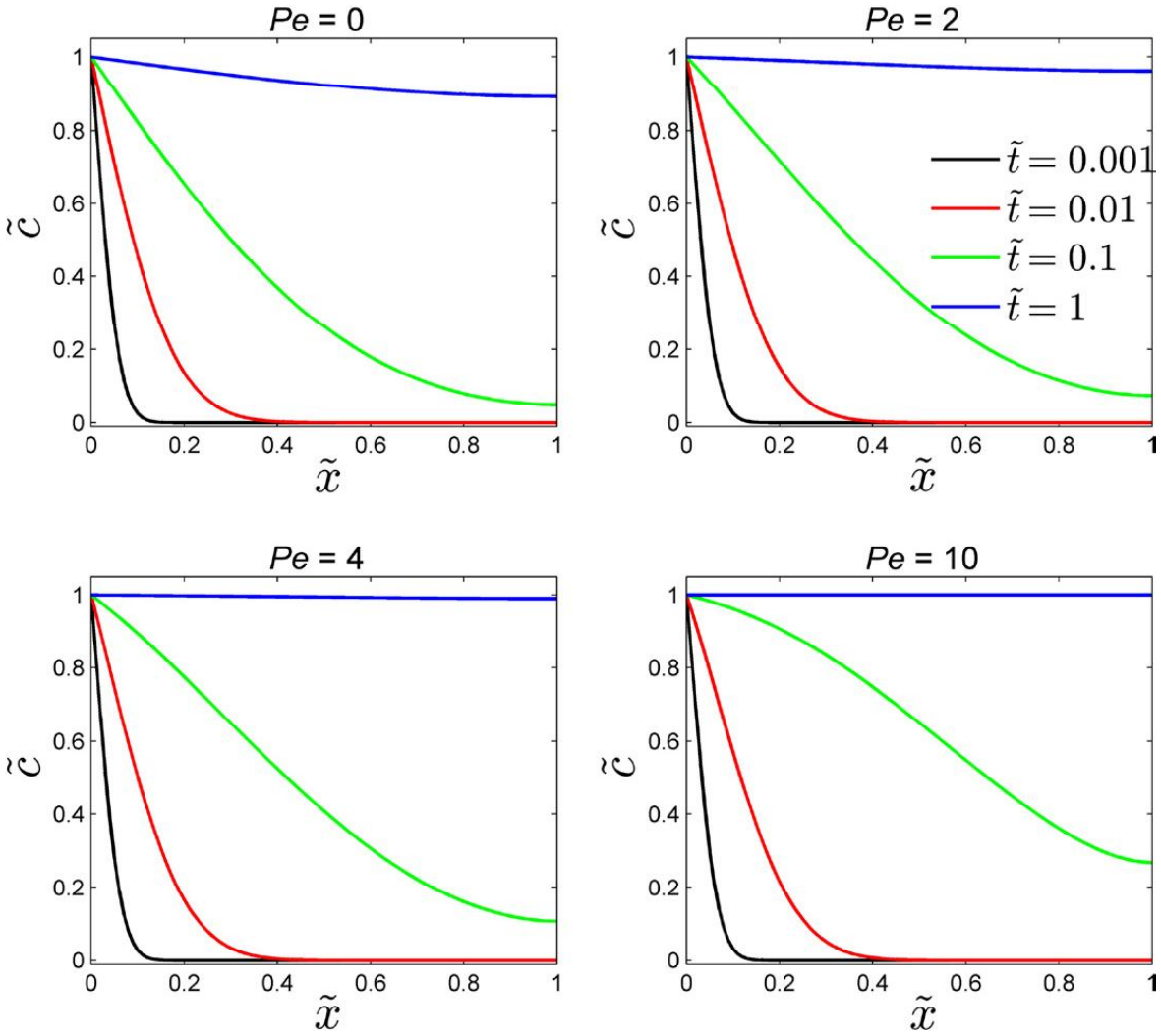

FIGURE 3.11 Transient concentration solutions for 4 different Péclet numbers.

3.6 APPLICATIONS OF POROUS MEDIA TO THE DRUG-ELUTING STENT

This section describes a very common procedure that involves the application of porous media to the previously discussed LME theory. The subject of this particular application involves what is referred to as the drug-eluting stent (DES).

As was already discussed in Section 3.1, the alteration of blood flows due to the narrowing (stenosis) or occlusion of an artery is one of the most common occurrences in cardiovascular diseases. Among the various available medical treatments, a well-established technique regards the insertion into the artery of a wired scaffold, or stent. The stent is designed to

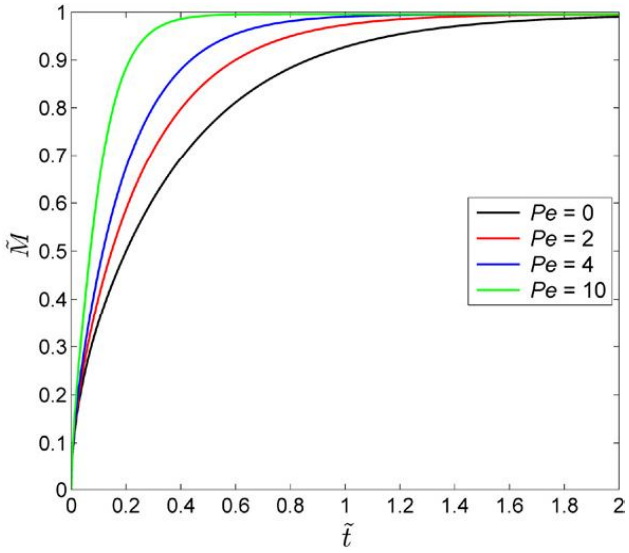

FIGURE 3.12 Drug mass versus time with Péclet number as a parameter.

mechanically provide the structural stability required to hold open the injured vessel in order to restore the correct blood flow. A typical design of the scaffold itself is provided in Fig. 3.13, and this metallic mesh is placed directly into the inner lining of the injured vessel. A challenge to the long term effectiveness of this treatment, however, has been reported, due to the tendency for tissue to grow around the scaffold's wire structure over time, thus recreating the blockage and re-occluding the lumen [4]. A solution to this is chemical inhibition of this growth by a local and controlled delivery of drugs. To ensure that the delivery is localized, the drug is contained within a very thin, porous, polymeric layer coating of the stent's surface. This design is known as the drug-eluting stent (DES), and its application has been targeted at healing the vascular tissues, and at preventing possible restenosis by virtue of its anti-proliferative action against smooth muscle cells. The application of the DES is an emerging technology that combines mechanical support of restricted lumen with local drug delivery [3,4], and although different configurations exist, a typical DES consists of the metallic strut, coated with one or more biocompatible polymeric layers containing the therapeutic agent to be delivered [36,37].

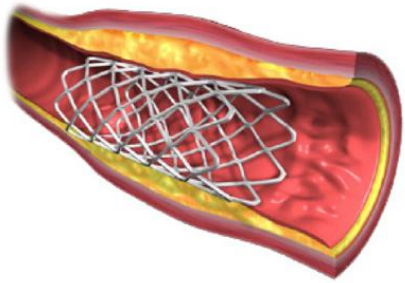

FIGURE 3.13 Metallic mesh of a stent implanted in a stenotic artery.

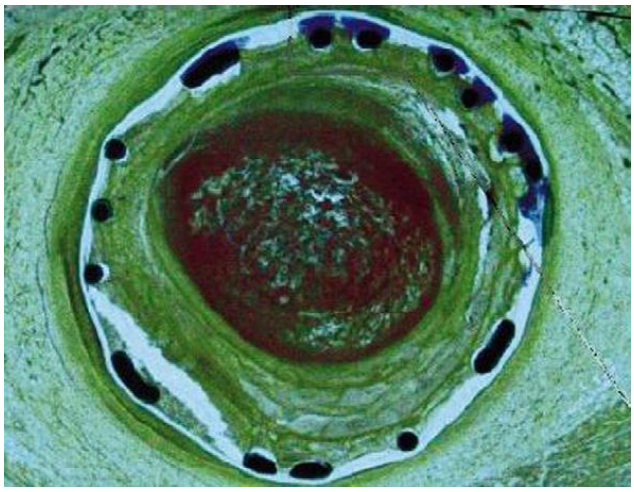

FIGURE 3.14 Section of a stented artery with the struts (in black) embedded into the wall.

Recently, polymeric gels have become much more prominent in their use as drug carrier devices in many biotechnological applications [38]. When designing these porous media, a drug-filled gel is stored within a solid polymer matrix, which enables the diffusive delivery of the drug to the surrounding tissue. With this in mind, the growth-inhibiting drug is loaded into a polymeric gel matrix that is added to the metallic struts of the stent. This allows slow, controlled, drug release after the stent has been implanted. In typical designs, the stent struts are uniformly covered by the polymer, and this is referred to as a coated stent. In an alternative design, honeycombed strut elements are inlaid with the polymer gel (stent with drug reservoirs, shown in Fig. 3.14) [39].

It is important to understand the dynamic nature of the delivery, because, while the drug concentration should meet some minimum requirement in order to achieve its desired effect, exceeding a critical threshold concentration may produce a toxic effect resulting in the destruction of tissue [40]. The drug is released through the vessel wall by both convective and diffusive processes. However, the theoretical understanding of the local transport is further complicated by the potential of metabolism of the drug by the surrounding tissue. Furthermore, it is likely that transport is locally impeded by partitioning at the interface of different tissue types that make up the arterial wall. The dynamic design of DES is aimed at the prolonged release of the drug and controlled delivery to the surrounding tissue, and mathematical models have been proposed to simulate the complex physics underlying the transient transport of the drug from the stent and into the arterial wall.

Drug release and transport depend on many of the geometric and physical parameters related to the drug, the stent, and the tissue making up the arterial wall [41]. Computational modeling has been shown to provide remarkable insight into the physical factors that influence the delivery process. These include the geometrical design of the stent, the mechanical characteristics of the materials and the chemical properties of the drug [42]. These effects play out over different time and space scales and, in order to illuminate the underlying physics associated with the drug's deposition, integrative biomechanical methods are required [43]. Recently, a number of mathematical models have been developed that address the

fundamental problem of the mass release from DES through the arterial wall [5,6,44,45]. Unconventional approaches of drug delivery, such as those based on the endoluminal gel paving technology, have been recently proposed [46]. Multi-physics studies incorporating the principles of solid and fluid mechanics are able to capture both the mechanical expansion of the strut as well as the DES elution properties [47]. Difficulties in coupling different geometrical scales have been reported [48], and solutions have recently been proposed that incorporate multiscale modeling strategies [49].

Mathematical descriptions of the system can be categorized according to the level of complexity of the arterial wall description and, according to *Prosi et al.* [48], there are three cases into which these models fall.

- The simplest and least descriptive of these is the wall-free model which describes the entire arterial wall through boundary conditions. While this straightforward approach is easily implemented, unfortunately all information involving any spatial variation drug concentration within the arterial wall is lost.
- The fluid wall model approximates the wall structure as a single homogeneous layer. In many studies, the complex composite nature of the multi-layered structure making up the arterial wall is disregarded and, instead, porous media theory is used to depict the physical domain by a homogenous, spatially averaged representation. This approach has been used with great success in numerical and analytical studies of DES behavior [5,50]. Although the fluid wall model is more accurate than the wall-free model, its inherent integrative approach to the description of the arterial wall is unable to capture the role that discontinuities within the tissue microstructure can play in the drug release mechanism.
- The motivation of the multi-layered wall model is based on the knowledge that the actual anatomy of the arterial wall is known to be composed of multiple layers, each with its own distinct structural and chemical properties [50,51]. Furthermore, it is well accepted that a more accurate description of the drug delivery requires a realistic depiction of the wall structure. The multi-layered model is the most complete model, and takes into account the heterogeneous nature of the composite structure of the arterial wall: that each layer has its own distinct properties, and thus that the drug's behavior in each layer is distinct as well. However, due to its composite nature, the multi-layered wall has a high potential for producing very complicated and algebraically involved solutions.

The choice between the fluid wall model and the multi-layered wall model is made by considering the tradeoff between the required level of detail of the solution, the availability of data describing the physical parameter values and the acceptable degree of solution complexity. The multi-layer model is more comprehensive than the fluid wall model because it can provide a detailed description of the inter-tissue drug behavior. However, it should come as no surprise that with each additional layer the complexity of the solution increases. Furthermore, in order to present an accurate portrayal of the drug's behavior as it passes through the multi-layered domain, knowledge of the parameter values that characterize the physical properties of each layer must be available. For this reason, the analytical solutions of both the fluid wall model and the multi-layered model are provided in the next subsections.

These solutions have been derived under the simplifying assumption of one-dimensional transport of the drug. In addition, as the drug is initially contained only in the solid polymeric

matrix of the coating, whose pores (channels) are occupied by the plasma after DES implantation, at $t = 0$ we have $c^s(x, t = 0) = C^s_{f0}$ and $c^f(x, t = 0) = 0$. Strictly speaking, it is not acceptable to assume a LME, so that $c^f = c^s = c$ in Eqs. (3.27a) and (3.28a), as shown in 3.5. However, to simplify the analysis, it is here assumed that at $t = 0$ the drug mass is instantaneously transferred to the fluid phase from the solid matrix and, then, released into the arterial wall. Hence, $c^f(x, t = 0) = C^s_{f0}$ and the solid gel can be completely neglected. This simplifying assumption is removed in [52] where a two-phase model is considered.

3.6.1 The Fluid Wall Model: The Pure Diffusion Approximation

The fluid wall model eliminates some of the inherent complexities associated with the composite nature of the arterial wall by using a single layer whose homogenous physical properties represent the combined effects of the multiple layers of the actual artery [39,48].

This simplistic model will be extended in the next sections to include more general effects and wall structure, but its description provides the methodological framework used. The analytical studies [5] use the fluid wall model approximation in conjunction with porous media representations of both the coating and the arterial wall in order to successfully provide a parametric analysis. The solution of that study, which is summarized in this section, provides an excellent tool for analysis in order to develop a better understand the underlying physics of DES delivery.

3.6.1.1 General Physiological and Mathematical Description

The conceptual physical space of the fluid wall model of DES consists of two layers. The stent is coated with a polymeric gel that is represented by Layer 0 (of thickness l_0). The stent is embedded into the arterial wall (Layer 1 of thickness l_1), as illustrated in Fig. 3.15. Because the fluid wall approximation is being applied, the complex multi-layered structure of the arterial wall can be considered to behave homogeneously with averaged properties inside Layer 1. Both the coating and the arterial wall are treated as porous media [12].

Because most of the mass transport process occurs along the direction normal to the two layers (radial direction), we restrict our study to a simplified one-dimensional model. In particular, we consider the transient transport along a coordinate axis that crosses the metallic strut, the coating, and the arterial wall. The wall thickness is very small relative to the arterial radius, and thus the Cartesian coordinate system is used (see Fig. 3.15). Taking the perspective that applies to either the luminal or the adventitial side, the drug transport route originates within the stent's porous coating, and progresses into the arterial wall, so that the positive coordinate axis direction is oriented away from the stent surface and into the arterial wall.

A volume-averaged concentration of drug in the fluid phase $\bar{c}^f = \langle c^f \rangle$ is considered in place of the intrinsic volume-averaged concentration $c^f = \langle c^f \rangle^f$, that is related to the previous quantity by $c^f = \bar{c}^f / \varepsilon_k$ (Section 3.2.1.1). For the sake of brevity, $\bar{c}^f$ will henceforth simply be denoted by c. Because it is anticipated that the drug's behavior is distinct in each of the system's two porous layers, the drug behavior may be considered in terms of two distinct components: $c_0(x, t)$ which corresponds to the drug concentration in the polymeric gel of Layer 0, and $c_1(x, t)$ which corresponds to the drug concentration in the arterial wall of Layer 1.

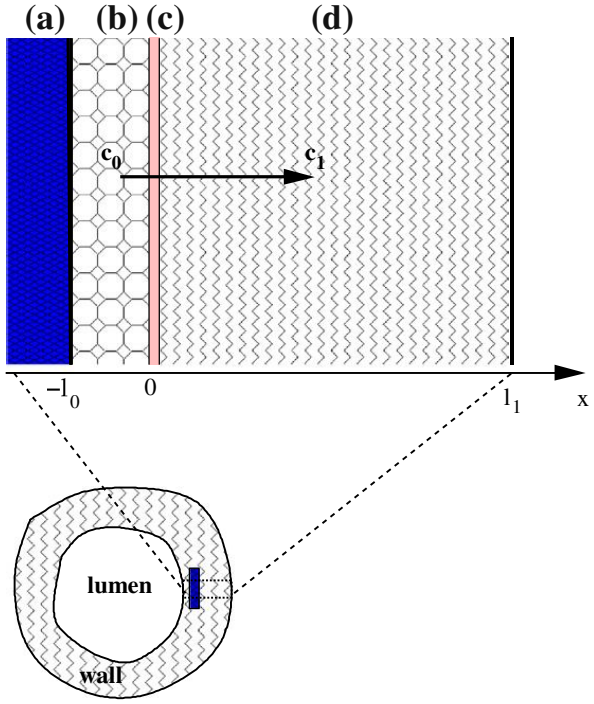

FIGURE 3.15 Cross section of a stented artery with a zoomed area near the wall that shows the metallic mesh and the two-layer medium at the adventitial side described by the model (3.68)–(3.70): (a) stent strut, (b) coating, (c) topcoat, (d) arterial wall. Due to an initial difference of concentration, drug is released in the arterial wall from (b) to (d) through the permeable membrane (c). An analogous two-layer pattern is present on the opposite side of the strut, referring to the drug dynamics towards the lumen (lumenal side).

As was already said, initially ($t = 0$) the drug mass is instantaneously transferred to the fluid phase from the solid matrix, and then released into the arterial wall. Hence, $c_0(x, t = 0) = C_0$ where C_0 is some uniform concentration value. Since the strut is impermeable to the drug, no mass flux passes through the boundary surface corresponding to the stent-coating interface at $x = -l_0$. Moreover, it is assumed that the plasma velocity through the pores of the polymeric gel matrix of the coating is very low after DES implantation, so that the drug transport in Layer 0 is governed by pure diffusion. Bearing in mind Eq. (3.27b), the dynamics of the drug in the fluid phase of the coating can be described by the following differential equations:

$$\frac{\partial c_0}{\partial t} = D_0 \frac{\partial^2 c_0}{\partial x^2} \quad (-l_0 < x < 0; t > 0) \tag{3.68a}$$

$$\left(\frac{\partial c_0}{\partial x}\right)_{x=-l_0} = 0 \quad (t > 0) \tag{3.68b}$$

$$c_0(x, t = 0) = C_0 \quad (-l_0 < x < 0) \tag{3.68c}$$

where D_0 is the effective diffusion coefficient of the drug in the fluid phase of the polymeric coating. Also, we recall that it is a volume-averaged quantity per unit volume of the fluid phase (intrinsic quantity), that is, $D_0 = \left\langle D^f_{d0} \right\rangle^f$, where the subscript d denotes drug while 0 indicates coating (Layer 0).

As implied in the discussion of the stent coating's initial condition, an equally valid assumption can be that initially no drug is present in the tissue of the arterial wall. A zero concentration can be prescribed at the domain boundaries of the artery on both the luminal side and the adventitial side. This is justified as follows. Because the arterial wall of the adventitial side is much thicker than the strut coating ($l_1 \gg l_0$), the concentration c_1 at $x = l_1$ does not change with time, so that its initial zero value is preserved at that location. In the case of the lumenal side, the position $x = l_1$ corresponds to the interface between the arterial wall and the blood stream. Because of the extremely high mass transfer coefficient of the blood stream (washout), it is reasonable to assume that the concentration at this point is zero.

It should be noted that in both cases, this homogeneous boundary condition of the first kind at $x = l_1$ will result in a fraction of drug being transported out of the arterial wall and into the tissues adjacent to the adventitia, or on the luminal side, a fraction of the drug will be dispersed into the lumen side blood stream. Once it has been transported out of the arterial wall, these fractions of the drug are considered as 'lost', because that component of the drug is no longer available to treat the tissues of the arterial wall.

In the wall (Layer 1), the drug dynamics are described by the following equation and related boundary/initial conditions:

$$\frac{\partial c_1}{\partial t} = D_1 \frac{\partial^2 c_1}{\partial x^2} \quad (0 < x < l_1; t > 0) \tag{3.69a}$$

$$c_1(x = l_1, t) = 0 \quad (t > 0) \tag{3.69b}$$

$$c_1(x, t = 0) = 0 \quad (0 < x < l_1) \tag{3.69c}$$

where D_1 is the effective diffusion coefficient of the drug in the fluid phase of the arterial wall.

This representation of the transport is extremely simple, primarily because it neglects any advection that would be associated with the flow of plasma within the wall tissue. This equation also neglects any uptake of the drug by the arterial lining. Similar assumptions are described in [5] and, while this has been shown to provide reasonable results, in the next subsection (Section 3.6.2) we develop a more comprehensive model including both advection and drug reaction.

To close the system of Eqs. (3.68) and (3.69), the conditions at the interface $x = 0$ (the so-called inner boundary conditions) have to be assigned. One of them is obtained by imposing continuity of the mass flux at the interface:

$$D_0 \left(\frac{\partial c_0}{\partial x} \right)_{x=0} = D_1 \left(\frac{\partial c_1}{\partial x} \right)_{x=0} \quad (t > 0) \tag{3.70a}$$

Now consider that, in order to slow down the drug release rate, a permeable membrane (called the topcoat) of permeability P is used to cover the surface of the drug-filled coating of Layer 0. In our model, the topcoat is located at the interface ($x = 0$) between the coating and the

arterial wall, as shown in Fig. 3.15. The topcoat is sufficiently thin (even relative to Layer 0) that its interfacial resistance can be represented by a jump discontinuity in concentration at the interface. To do this, the mass transfer through the topcoat can be described using the second Kedem-Katchalsky equation (see Subsection 9.3.3 of [15,39,48,53]). Thus, the continuous flux of mass passing across the membrane normally to the coating may be expressed by:

$$-D_0\left(\frac{\partial c_0}{\partial x}\right)_{x=0} = P\left[\frac{c_0(0,t)}{\varepsilon_{k,0}} - \frac{c_1(0,t)}{\varepsilon_{k,1}}\right] \quad (t>0) \tag{3.70b}$$

A generalized form of the above equation, including the effect of the boundary layers formed on either side of the membrane on the volume and solute fluxes, was derived in [54].

3.6.1.2 *Concentration Solutions and Results*

Using the following dimensionless transformations:

$$\begin{aligned} &\tilde{x} = \frac{x}{l_1}, \quad \tilde{t} = \frac{D_1}{l_1^2}t, \quad \tilde{c}_0 = \frac{c_0}{C_0}, \quad \tilde{c}_1 = \frac{c_1}{C_0} \\ &\gamma_0 = \frac{D_0}{D_1}, \quad \tilde{l}_0 = \frac{l_0}{l_1}, \quad \phi = \frac{Pl_1}{D_1\varepsilon_{k,1}}, \quad \sigma_0 = \frac{\varepsilon_{k,0}}{\varepsilon_{k,1}} \end{aligned} \tag{3.71}$$

and by re-setting the variables:

$$\tilde{x} \to x, \quad \tilde{t} \to t, \quad \tilde{c}_0 \to c_0, \quad \tilde{c}_1 \to c_1, \quad \tilde{l}_0 \to l_0 \tag{3.72}$$

the governing Eqs. (3.68)–(3.70) given in the previous subsection may be represented in a dimensionless form as:

$$\frac{\partial c_0}{\partial t} = \gamma_0\frac{\partial^2 c_0}{\partial x^2} \quad (-l_0 < x < 0; t>0) \tag{3.73a}$$

$$\left(\frac{\partial c_0}{\partial x}\right)_{x=-l_0} = 0 \quad (t>0) \tag{3.73b}$$

$$\gamma_0\left(\frac{\partial c_0}{\partial x}\right)_{x=0} = \left(\frac{\partial c_1}{\partial x}\right)_{x=0} \quad (t>0) \tag{3.73c}$$

$$c_0(x,t=0) = 1 \quad (-l_0 < x < 0) \tag{3.73d}$$

and:

$$\frac{\partial c_1}{\partial t} = \frac{\partial^2 c_1}{\partial x^2} \quad (0 < x < 1; t>0) \tag{3.74a}$$

$$-\gamma_0\left(\frac{\partial c_0}{\partial x}\right)_{x=0} = \phi\left[\frac{c_0(0,t)}{\sigma_0} - c_1(0,t)\right] \quad (t>0) \tag{3.74b}$$

$$c_1(x=1,t)=0 \quad (t>0) \tag{3.74c}$$

$$c_1(x,t=0)=0 \quad (0<x<1) \tag{3.74d}$$

The initial boundary value problem of Eqs. (3.73) and (3.74) is similar to the problem of heat diffusion in a two-layer slab. The analytical solution to this problem has been developed for the transient diffusion of mass associated with the DES in the study [5] by using the Separation of Variables (SOV) method. The solution is presented as follows.

The non-dimensional concentrations are represented by the Fourier series solutions:

$$c_0(x,t)=\sum_{m=1}^{\infty} A_m X_{0m}(x)\exp\left(-\gamma_0\lambda_{0m}^2 t\right) \quad (-l_0\le x\le 0;\, t\ge 0) \tag{3.75a}$$

$$c_1(x,t)=\sum_{m=1}^{\infty} A_m X_{1m}(x)\exp\left(-\lambda_{1m}^2 t\right) \quad (0\le x\le 1;\, t\ge 0) \tag{3.75b}$$

where the two layers' eigenvalues λ_{0m} and λ_{1m} are related by the relation $\lambda_{0m}=\lambda_{1m}/\sqrt{\gamma_0}$.

Also, the corresponding eigenfunctions are represented by:

$$X_{0m}(x)=a_{0m}\cos\left(\lambda_{0m}x\right)+b_{0m}\sin\left(\lambda_{0m}x\right) \quad (-l_0\le x\le 0) \tag{3.76a}$$

$$X_{1m}(x)=a_{1m}\cos\left(\lambda_{1m}x\right)+\sin\left(\lambda_{1m}x\right) \quad (0\le x\le 1) \tag{3.76b}$$

for which:

$$a_{0m}=-\sigma_0\left[\frac{\lambda_{1m}}{\phi}+\tan\left(\lambda_{1m}\right)\right] \quad b_{0m}=\frac{1}{\sqrt{\gamma_0}} \quad a_{1m}=-\tan\left(\lambda_{1m}\right) \tag{3.77}$$

Each of the terms of the series of solution of Eq. (3.75) has an eigenvalue associated with it. The closure of the components of the solution, Eqs. (3.76)–(3.77), requires the value of each of the 'm' eigenvalues ($m=1, 2, \ldots$) of Layer 1, λ_{1m}. These are evaluated numerically as roots of the transcendental equation (eigencondition), $a_0\tan\left(\lambda_0 l_0\right)+b_0=0$, that is:

$$\underbrace{\sigma_0\left[\frac{\lambda_1}{\phi}+\tan\left(\lambda_1\right)\right]}_{-a_0}\tan\left(\frac{l_0}{\sqrt{\gamma_0}}\lambda_1\right)-\underbrace{\frac{1}{\sqrt{\gamma_0}}}_{b_0}=0 \tag{3.78}$$

Then, by appying the initial condition, the constant of integration appearing in Eqs. (3.75) is evaluated as $A_m=-b_{0m}/(N_m\lambda_{0m})$, where the dimensionless norm N_m coming from the orthogonality property of the eigenfunctions is given by (see App. 5 of Ref. [5]):

$$N_m=\frac{1}{2}\left[\left(a_{0m}^2+\frac{1}{\gamma_0}\right)l_0-\frac{a_{0m}}{\lambda_{1m}}+\sigma_0\left(a_{1m}^2+1-\frac{a_{1m}}{\lambda_{1m}}\right)\right] \tag{3.79}$$

For a discussion of the determination of the eigenvalues and the sensitivity of the solution to the number of terms in Eqs. (3.75), the reader is encouraged to consider the study [5]. In that study, dimensionless parameter values are used which are made up of the dimensional parameter values that are representative of a typical DES. These parameters have been chosen on a physical basis and in agreement with the typical scales in DES and data in literature for the arterial wall and heparin drug in the coating layer ([40,42,55]). The resulting parameter values:

$$\phi = 0.234, \quad \sigma_0 = 0.164, \quad l_0 = 0.05, \quad \gamma_0 = 0.0014 \tag{3.80}$$

are used to develop the solution and to evaluate the eigenvalues that are the roots of Eq. (3.79). The concentration profiles for three values of dimensionless time are displayed in Fig. 3.16. The drug elutes from the coating to the wall, with its concentration decaying over time. Because of the different properties of the two layers, at early times the concentrations exhibit very steep gradients near $x = 0$, which disappears at later times.

To present a more globalized, transient depiction of the process, that study introduces the concept of the instantaneous dimensionless drug mass per unit area, $\tilde{M}_i = M_i/C_0 l_1$, present in both the coating ($i = 0$) and the arterial wall ($i = 1$) layers. By re-setting $\tilde{M}_i \to M_i$, these masses are defined as:

$$M_0(t) = \int_{-l_0}^{0} c_0(x,t)dx = \sum_{m=1}^{\infty} A_m^2 N_m \exp(-\lambda_{1m}^2 t) \tag{3.81a}$$

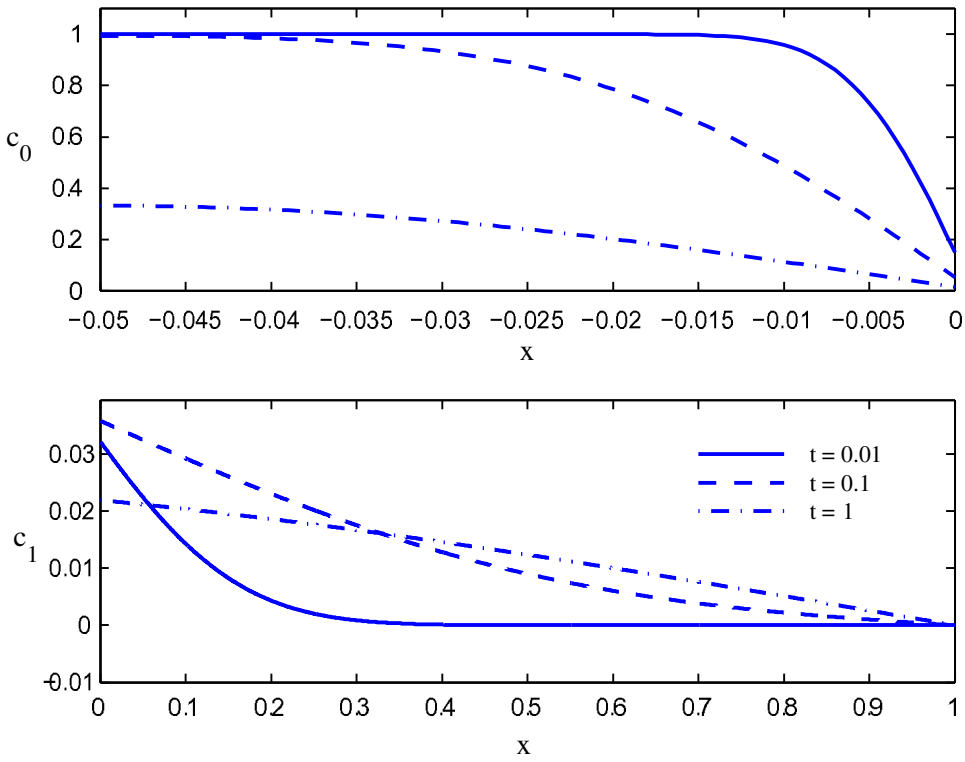

FIGURE 3.16 Drug concentration profiles in the coating (above) and in the wall (below) for three different times (note the different space scales).

$$M_1(t) = \int_0^1 c_1(x,t)dx = \sum_{m=1}^{\infty} A_m \frac{\cos(\lambda_{1m}) - 1}{\lambda_{1m}\cos(\lambda_{1m})} \exp(-\lambda_{1m}^2 t) \tag{3.81b}$$

Figure 3.17 shows that the drug mass in the coating layer, M_0, decreases monotonically, while the mass in the wall, M_1, first increases to a maximum M_1^* at time t^*, then decreases to zero at the same rate as M_0. Since the drug is absorbed at $x = 1$, the total mass is not preserved and tends to zero at very large times.

In principle, the drug diffusion occurs from the coating towards both the lumen (inner wall) as well as towards the adventitia (outer wall). Therefore an inner two-layer system (lumenal side) and an outer two-layer system (adventitial side) should be distinguished. The relative importance of the transport in either direction depends on the penetration depth of the stent. The adventitial side is generally larger in size and deemed more relevant from a clinical point of view. However, it should be noted that the methodology and solution formulation presented in this section are general and apply to transport in both the inner (lumenal) and outer (adventitial) sides of the stent.

3.6.2 The Fluid Wall Model: The Advection-Reaction-Diffusion Equation

The previous solution does not consider the effects of the plasma flow through the tissues composing the arterial wall. While this assumption has been shown to hold using scale analysis [5] as well as numerical models [39], the description of the fluid wall model of the

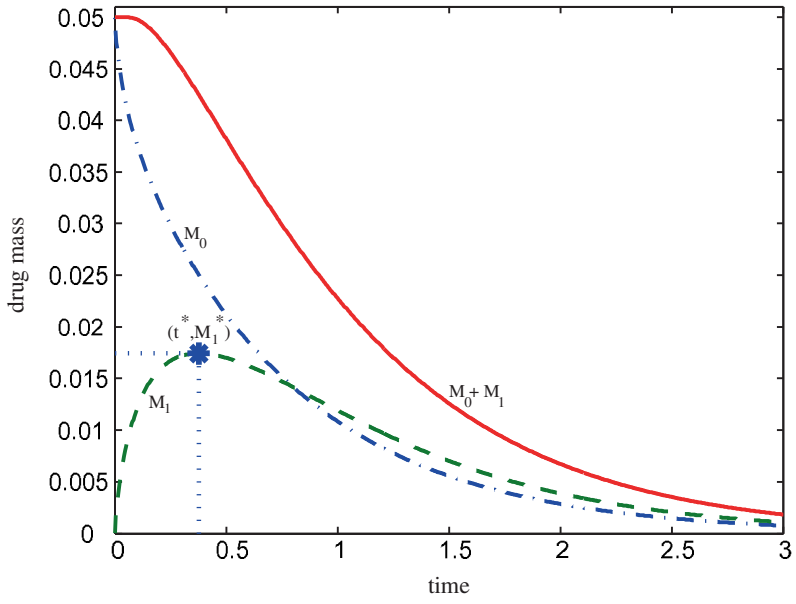

FIGURE 3.17 Dimensionless drug mass in the coating (- · - · -), in the wall (- - -) and total mass (—) as function of time. In the coating, drug mass M_0 is monotonically decreasing, while in the wall there is a characteristic time t^* at which the drug reaches a maximum peak M_1^*. Due to the absorption at the wall side, drug is not preserved and vanishes at a time large enough.

DES is not complete without considering this phenomenon. This section develops the governing equations, boundary and interface conditions and presents the solution of the drug deposition from the DES that includes the advective contribution within the arterial wall as well as the uptake of the drug by the arterial wall tissue. Referring once more to Fig. 3.15, and recalling that the adventitial side is generally larger in size and deemed more relevant from a clinical point of view, the following discussion will only consider the transport from the stent to the outer arterial wall (adventitial side).

3.6.2.1 *General Physiological and Mathematical Description*

Following the coordinate system presented in Fig. 3.15, we first consider the solute within the stent's thin porous coating. Initially, the drug is contained only in the fluid phase of the stent thin porous coating, and the initial concentration is represented by a potentially non-uniform distribution, $C_0 \cdot F_0(x)$, where C_0 is a constant and $F_0(x)$ is an arbitrary dimensionless function such that $0 \leq F_0(x) \leq 1$. Again, the strut is impermeable to the drug, so no mass passes through the boundary surface corresponding to the stent-coating interface at $x = -l_0$. Transport in Layer 0 is governed by pure diffusion because the velocity of plasma penetrating into the stent's coating is very low. Thus, the dynamics of the drug in the fluid phase of the coating (Layer 0) is still described by Eqs. (3.68a)–(3.68c), and only the initial condition is now different.

In the wall (Layer 1), bearing in mind Eq. (3.27b), the drug dynamics are described by the following advection-reaction-diffusion equation:

$$\frac{\partial c_1}{\partial t} = D_1 \frac{\partial^2 c_1}{\partial x^2} - 2\delta_1 \frac{\partial c_1}{\partial x} - \beta_1 c_1 \quad (0 < x < l_1; t > 0) \tag{3.82}$$

where the advective component is represented by the parameter $2\delta_1 = f_1 u_1 / \varepsilon_{k,l}$.

The quantity $f_1 u_1$ is the drug velocity in the arterial wall, which has been considered to be uniform and constant. In particular, the term f_1 is the retardation coefficient defined in Section 3.3.1 (also known as the hindrance coefficient) and u_1 is the plasma velocity. For an isothermal and incompressible fluid in a porous medium, the local flow velocity u_1 may be calculated by Eq. (3.10). Note that the advective component is sometimes represented as $2\delta_1 = (1 - v_1)u_1$, where $v_1 = 1 - f_1/\varepsilon_{k,l}$ is known as the Stavernan filtration coefficient [56].

The last term on the left-hand side of Eq. (3.82) represents the drug reaction inside the media layer of the arterial wall. Here, it is approximated by a linear reaction having $\beta(> 0)$ as an effective first-order consumption rate coefficient. The boundary and initial conditions associated with Eq. (3.82) are still defined by Eqs. (3.69b) and (3.69c), respectively. To close the mass transfer system of defining equations, the conditions at the interface ($x = 0$) will now be assigned. One of them is obtained by imposing continuity of the mass flux across the two layers as expressed by Eq. (3.70a). For the current purposes, it is rewritten as:

$$D_0 \left(\frac{\partial c_0}{\partial x} \right)_{x=0} = D_1 \left(\frac{\partial c_1}{\partial x} \right)_{x=0} - 2\delta_1 c_1(0,t) \quad (t > 0) \tag{3.83}$$

The interfacial resistance due to the transport inhibiting influence of the topcoat coating of Layer 0 is again represented by the second Kedem-Katchalsky equation, i.e., Eq. (3.70b).

3.6.2.2 *Concentration Solutions and Results*

In order to represent the system in non-dimensional terms, the same dimensionless variables previously listed in Eq. (3.71) can be used. When this is done, the convection and reaction terms are represented by:

$$Pe = \frac{\delta_1 l_1}{D_1} \quad \Phi = \sqrt{\frac{\beta_1 l_1^2}{D_1}} \tag{3.84}$$

The Péclet number, Pe, expresses the ratio of the transport of the drug by advection to the diffusion of the drug within the arterial wall. The Thiele modulus, Φ, is a dimensionless number characterizing the ratio of the reaction rate to the diffusion rate [53].

The dimensionless variables can then be rewritten as in Eq. (3.72) to simplify the solution presentation. In order to resolve the solution at the interface, the following transformation of Layer 1 is performed which was suggested by *Özişik* (see Eq. (2–168) on p. 90 of Ref. [57]):

$$c_1(x,t) = w_1(x,t)\exp[Pe \cdot x - (Pe^2 + \Phi^2)t] \tag{3.85}$$

The governing equations of the current problem may be represented in dimensionless form as:

$$\frac{\partial c_0}{\partial t} = \gamma_0 \frac{\partial^2 c_0}{\partial x^2} \quad (-l_0 < x < 0; t > 0) \tag{3.86a}$$

$$\left(\frac{\partial c_0}{\partial x}\right)_{x=-l_0} = 0 \quad (t > 0) \tag{3.86b}$$

$$\gamma_0 \left(\frac{\partial c_0}{\partial x}\right)_{x=0} = \left[\left(\frac{\partial w_1}{\partial x}\right)_{x=0} - Pe \cdot w_1(0,t)\right] \exp\left[-(Pe^2 + \Phi^2)t\right] \quad (t > 0) \tag{3.86c}$$

$$c_0(x, t=0) = F_0(x) \quad (-l_0 < x < 0) \tag{3.86d}$$

and:

$$\frac{\partial w_1}{\partial t} = \frac{\partial^2 w_1}{\partial x^2} \quad (0 < x < 1; t > 0) \tag{3.87a}$$

$$-\gamma_0 \left(\frac{\partial c_0}{\partial x}\right)_{x=0} = \phi \left\{\frac{c_0(0,t)}{\sigma_0} - w_1(0,t)\exp[-(Pe^2 + \Phi^2)t]\right\} \quad (t > 0) \tag{3.87b}$$

$$w_1(x=1,t) = 0 \quad (t > 0) \tag{3.87c}$$

$$w_1(x, t=0) = 0 \quad (0 < x < 1) \tag{3.87d}$$

The analytical solution to the above initial boundary value problem has been developed for the transient diffusion-advection of mass associated with the DES in the study [31] by using the SOV method. The solution is presented as follows.

The non-dimensional concentrations are represented by the Fourier series solutions:

$$c_0(x,t) = \sum_{m=1}^{\infty} A_m X_{0m}(x) \exp(-\gamma_0 \lambda_{0m}^2 t) \quad (-l_0 \le x \le 0; t \ge 0) \tag{3.88a}$$

$$c_1(x,t) = \exp[Pe \cdot x] \sum_{m=1}^{\infty} A_m X_{1m}(x) \exp\left[-(\lambda_{1m}^2 + Pe^2 + \Phi^2)t\right] \quad (0 \le x \le 1; t \ge 0) \tag{3.88b}$$

where the two layers' eigenvalues are related by the relationship $\gamma_0 \lambda_{0m}^2 = \lambda_{1m}^2 + Pe^2 + \Phi^2$, while the eigenfunctions are still represented by Eqs. (3.76) but with a different expression for their coefficients. We have:

$$a_{0m} = -\sigma_0 \left(1 + \frac{Pe}{\phi}\right) \left[\frac{\lambda_{1m}}{\phi + Pe} + \tan(\lambda_{1m})\right] \tag{3.89a}$$

$$b_{0m} = \frac{1}{\sqrt{\gamma_0}} \frac{\lambda_{1m} + Pe \tan(\lambda_{1m})}{\sqrt{\lambda_{1m}^2 + Pe^2 + \Phi^2}} \tag{3.89b}$$

$$a_{1m} = -\tan(\lambda_{1m}) \tag{3.89c}$$

where the eigenvalues λ_{1m} of Layer 1 may be determined by computing the roots of the transcendental equation (eigencondition), $a_0 \tan(\lambda_0 l_0) + b_0 = 0$, that is:

$$\underbrace{\sigma_0 \left(1 + \frac{Pe}{\phi}\right) \left[\frac{\lambda_1}{\phi + Pe} + \tan(\lambda_1)\right]}_{-a_0} \tan\left(\frac{l_0}{\sqrt{\gamma_0}} \sqrt{\lambda_1^2 + Pe^2 + \Phi^2}\right) - \underbrace{\frac{1}{\sqrt{\gamma_0}} \frac{\lambda_1 + Pe \tan(\lambda_1)}{\sqrt{\lambda_1^2 + Pe^2 + \Phi^2}}}_{b_0} = 0 \tag{3.90}$$

In this way each of the 'm' roots of Eq. (3.90) are used to develop a corresponding term of the series of the solution, Eqs. (3.88). These roots are in general real, but imaginary roots are possible too. Note that, when $Pe = 0$ and $\Phi = 0$, Eq. (3.90) reduces exactly to Eq. (3.78). Similarly, the coefficients defined by Eqs. (3.89) reduce to the ones given by Eqs. (3.77).

In Eq. (3.88) the constant of integration, A_m, is evaluated as:

$$A_m = \frac{1}{N_m} \int_{x=-l_0}^{0} F_0(x) X_{0m}(x) dx \tag{3.91}$$

which for the special case of a Layer 0 uniform initial distribution, $F_0(x) = 1$, may be expressed as $A_m = -b_{0m}/(N_m\lambda_{0m})$. The normalizing constant (norm), N_m, is defined by:

$$N_m = \frac{1}{2}\left[(a_{0m}^2 + b_{0m}^2)l_0 - \frac{a_{0m}b_{0m}}{\lambda_{0m}} + \sigma_0\left(a_{1m}^2 + 1 - \frac{a_{1m}}{\lambda_{1m}}\right)\right] \tag{3.92}$$

In the study in [31], a parametric investigation is conducted regarding the effects of the advection of the drug within the arterial wall, which in this solution is represented by the Péclet number, *Pe*. The study also examines the relative role of the drug reaction which is represented in the Thiele modulus, Φ. Using the dimensionless parameter values listed in Eq. (3.81), the concentration solution given by Eqs. (3.88) is plotted for different values of *Pe* and Φ. (In such a case, an imaginary eigenvalue was found.)

To show the influence of the filtration velocity on the drug release, a value $\delta_1 \cong 10^{-6} cm/s$ is considered, which reflects measurements presented in the studies in [47,58]. Simulations for four values of *Pe* in a compatible range have been carried out to show the trend of the solution. The effects on the drug transport within the arterial wall are plotted in Fig. 3.18. It is clear that introducing even a very small advective term lowers the concentration curves at all times. This is because the convection velocity sweeps the drug away from the wall, where it is dispersed. At intermediate and later instants, the profiles may appear bulged and therefore a more uniform concentration is guaranteed. A critical value of *Pe* exists; beyond it the solution no longer represents a physical reality.

The importance of the reaction term depends on the drug used, on the specific tissue and on individual factors. However, the presence of a reactive term acts as a sink for concentration. A typical value for the consumption rate coefficient is $\beta_1 \simeq 10^{-4}\, s^{-1}$ [59]. Consequently, $\Phi = \sqrt{0.15}$ and the trend of the concentration at three increasing values of Φ is depicted in Fig. 3.19. Increasing the value of Φ accelerates the drug consumption and diminishes the concentration, but preserves the shapes at fixed times. A negligible variation with Φ is reported at early times. At later instants, the concentration profiles flatten and decrease linearly. In conclusion, the effect on varying *Pe* is similar, though more sensitive, to that on Φ, and they combine when both coexist.

3.6.3 The Multi-Layered Wall Model: The Pure Diffusion Approximation

In this section, a multi-layered extension of pure diffusion model in Section 3.6.1 is developed. Following [50,60], an idealized model of wall consisting of four layers (namely endothelium, intima, internal elastic lamina and media) is proposed. Each layer is treated as a macroscopically homogeneous porous medium with its own distinct diffusion coefficient. A further simplification involves the endothelium that is covered by a thin ciliate layer called the *endothelial surface layer* or *glycocalyx* and this is composed of a sequence of long chain macromolecules and proteins [51]. As the drug transport properties through the glycocalyx are unknown, it has been included in the endothelium layer for simplicity. The stent coating is assumed to be a thin porous slab in imperfect contact with the endothelium due to the presence of a topcoat.

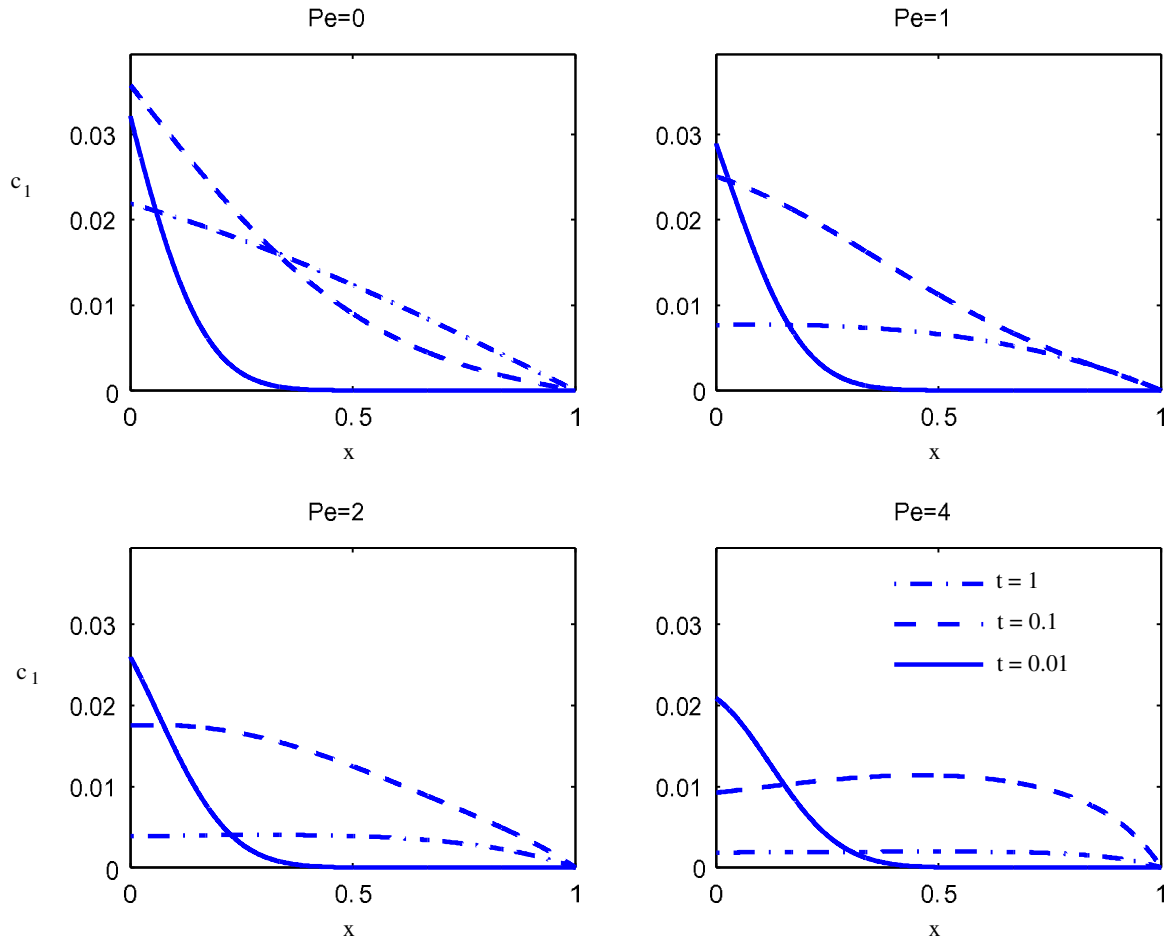

FIGURE 3.18 Wall concentration decay profiles at varying Pe (with $\Phi = 0$) for different locations and times.

3.6.3.1 *General Physiological and Mathematical Description*

The adventitia and the surrounding tissues form the outmost wall layer and have a sufficiently large extent to be considered as semi-infinite. The classical SOV method leads to a Sturm-Liouville problem with discontinuous coefficients and severe spectral irregularities. Drug concentration in each layer at various times is given in the form of a Fourier series by using dimensionless parameters which control the transfer mechanism across the layered wall. For generality, the problem is developed such that there is any number of arterial tissue layers.

First, consider a thin layer (of thickness l_0) of gel containing a drug that coats a stent which is embedded into the arterial wall [44]. Again we restrict our study to a simplified 1-D model and consider only the transport from the stent into the adventitial side arterial wall. In this way, the drug's behavior is considered along an outward pointing line crossing the metallic strut, the coating and the layers of the arterial wall. In a general 1-D framework, let us

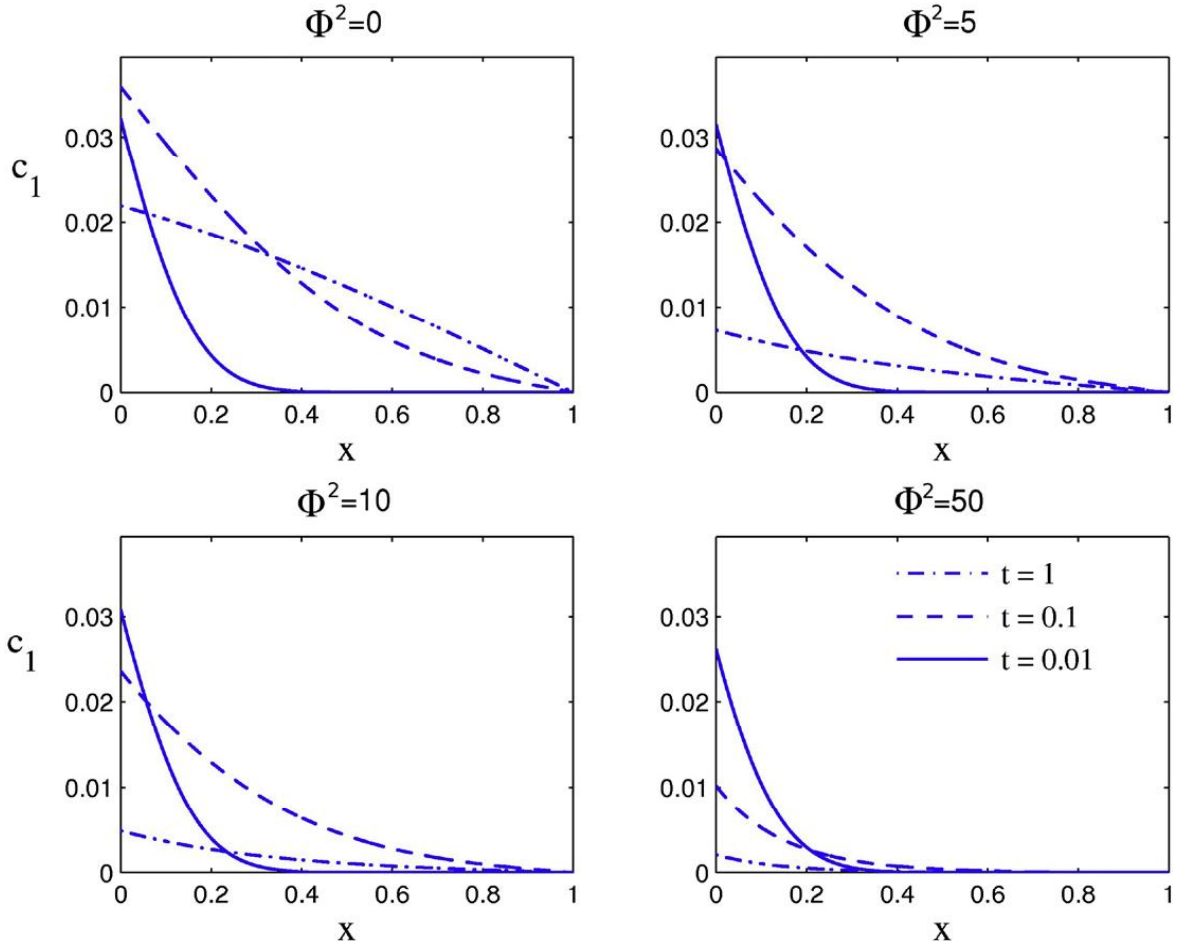

FIGURE 3.19 Wall concentration decay profiles at varying Φ (with $Pe = 0$) for different locations and times.

consider a set of intervals $[x_{i-1}, x_i]$ for $i = 0, 1, 2, \ldots, n$ each having thickness $l_i = x_i - x_{i-1}$ so that the coating (layer 0) and the wall layers (layers $i = 1, 2, \ldots, n$) are conceptually represented as in Fig. 3.20 where, without loss of generality, $x_0 = 0$ has been assumed to be the coating-wall interface.

At the initial time ($t = 0$), the drug is contained only in the plasma of the coating and it is distributed with a maximum, possibly non-uniform, concentration $C_0 \cdot F_0(x)$, with $0 \leq F_0(x) \leq 1$. Since the metallic strut is impermeable to the drug, no mass flux passes through the boundary surface $x = -l_0$. The dynamics of the drug in the coating (Layer 0) is described by a 1-D diffusion equation, and related boundary-initial conditions, as defined by Eqs. (3.68), where only the initial condition is now different, being non-uniform.

As reported in [50], the convection-reaction terms are only relevant in the media layer, whereas in the other layers these effects can be neglected. However, it has been shown in Section 3.6.2 that a more general model including convection-reaction terms can be reduced to a pure diffusive system by a variable transformation, namely Eq. (3.85). For this reason,

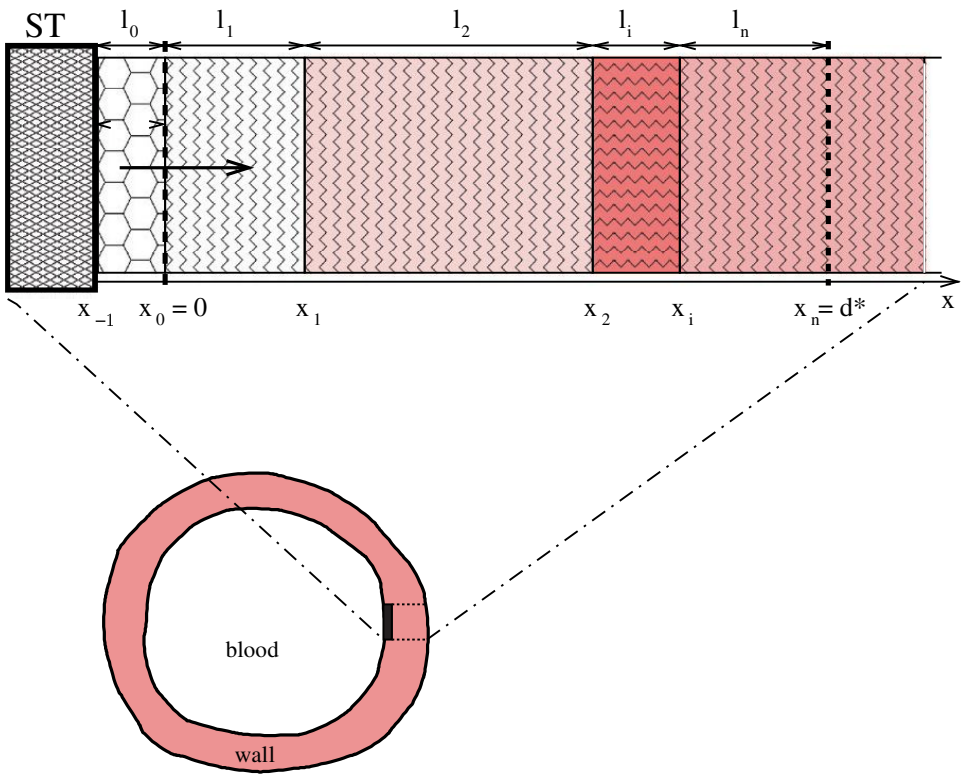

FIGURE 3.20 A sketch of the layered wall. The 1-D wall model is defined along the line normal to the strut stent surface and extends with a sequence of n contiguous layers $[x_{i-1}; x_i]$, $i = 1, 2, \ldots, n$ from the polymer coating interface $x_0 = 0$ up to the wall bound x_n estimated by the penetration distance d^*. ST indicates the metallic stent strut bearing the coating (figure not in scale).

within the $i = 1, 2, \ldots, n$ layers of the arterial wall, the drug dynamics are described by the following diffusion equation and related initial condition:

$$\frac{\partial c_i}{\partial t} = D_i \frac{\partial^2 c_i}{\partial x^2} \quad (x_{i-1} < x < x_i; t > 0) \tag{3.93a}$$

$$c_i(x, t = 0) = 0 \quad (x_{i-1} < x < x_i) \tag{3.93b}$$

where D_i is the effective diffusivity of the drug in the plasma of the ith layer of the arterial wall and c_i is the ith drug concentration.

At the interfaces between the layers of the arterial wall, the continuity of flux and the continuity of concentration relate the solutions of the $i = 1, 2, \ldots, n$ layers to one another:

$$D_i \left(\frac{\partial c}{\partial t}\right)_{x=x_i} = D_{i+1} \left(\frac{\partial c}{\partial x}\right)_{x=x_i} \quad (i = 1, 2, \ldots, n-1; t > 0) \tag{3.94a}$$

$$\frac{c_i(x_i, t)}{\varepsilon_{k,i}} = \frac{c_{i+1}(x_i, t)}{\varepsilon_{k,i+1}} \quad (i = 1, 2, \ldots, n-1; t > 0) \tag{3.94b}$$

As in the previous examples, the topcoat is used on the coating to slow the drug release into the arterial wall. This effect appears in the interface conditions between the coating (Layer 0) and the first tissue layer of the arterial wall (Layer 1), as indicated by Eqs. (3.70a) and (3.70b).

Finally, a boundary condition is imposed at the limit of the outermost tissue layer of the adventitia, x_n. Some controversy occurs when measuring this wall bound. Different values of the thickness are in fact given in the literature, depending on the arterial size; these generally lie in the range 100 to 200 μm for a medium sized artery [39,40,45,50]. Actually, as the arterial wall is embedded in the surrounding tissues, the drug transport does not suddenly stop at the outer limit of the adventitia but proceeds forward into the external tissues, and penetrates to a depth that depends on the time at which the process is observed. In principle, the exact range of the domain encompassing the diffusion process cannot be estimated *a priori*, and any truncation of the domain is rather arbitrary, if made on physiological considerations only. As a matter of fact, instead of arbitrarily guessing the correct wall thickness at which concentration and mass flux vanish asymptotically, a more rigorous approach may be made. This is done by modeling the outer boundary as a semi-infinite medium that is in perfect contact with the arterial media and having uniform properties (equal to those of the last layer, i.e., the adventitia) so that $x_n \to \infty$. The concentration and mass flux as $x \to \infty$ are finite (boundary condition of 0th kind or of Beck type; see Chap. 2 of Ref. [30]):

$$c_n(x \to \infty, t) = \text{finite}, \quad \left(\frac{\partial c_n}{\partial x}\right)_{x\to\infty} = \text{finite} \tag{3.95}$$

For computational purposes, it is possible to model the outmost layer within a bounded domain instead. This, in fact, is what has been suggested in [61], by using the concept of penetration distance d^*. Clearly the value of d^* increases with time and, in the case of a composite layered system, the penetration depth depends on the thickness and the diffusivities of each of the arterial wall layers. Also, it increases on the accuracy desired, for example 10^{-p}, with $p = 1, 2, \ldots, 10$. To estimate the penetration distance with which one can determine (with errors less than 10^{-p}) the outer bound of the outer arterial wall layer, x_n, the following estimate is provided in [60] as:

$$d^* \approx \sqrt{10pD_n t} + \sum_{j=1}^{n-1} l_j \left(1 - \delta_{ij}\right) \left(1 - \prod_{s=j}^{i-1} \sqrt{\frac{D_{s+1}}{D_s}}\right) \tag{3.96}$$

where δ_{ij} is the Kronecker delta.

Thus, without losing any significant accuracy, the nth semi-infinite layer can be truncated at the penetration distance, $x_n = d^*$, and the 0th kind boundary conditions (3.95) are replaced by:

$$c_n(x_n = d^*, t) = 0, \quad \left(\frac{\partial c_n}{\partial x}\right)_{x_n = d^*} = 0 \tag{3.97}$$

within an accuracy of 10^{-p}. In other words, setting condition (3.97) guarantees that the concentration and the mass flux vanish at d^* with a mass loss comparable with 10^{-p} at a given

time. In the outmost nth layer, both the above conditions hold, but the absorbing condition $c_n = 0$ is expected to be more realistic, since the vasa vasorum of the adventitia are continually replenished with fresh blood and sweep away any residual drug [45].

3.6.3.2 Concentration Solutions and Results

Using the following dimensionless variables:

$$\tilde{x} = \frac{x}{d^*}, \quad \tilde{t} = \frac{D_{\max}}{(d^*)^2}t, \quad \tilde{c}_i = \frac{c_i}{C_0}, \quad \tilde{l}_i = \frac{l_i}{d^*}$$
$$\gamma_i = \frac{D_i}{D_{\max}}, \quad \phi = \frac{Pd^*}{D_{\max}(\varepsilon_k)_{\max}}, \quad \sigma_i = \frac{(\varepsilon_k)_i}{(\varepsilon_k)_{\max}} \tag{3.98}$$

where the subscript *max* refers to the maximum value across the $n+1$ layers, and then by means of the change of variables of Eq. (3.72) (here adding $\tilde{l}_i \to l_i$), the drug balance equations are recast in a dimensionless form as:

$$\frac{\partial c_i}{\partial t} = \gamma_i \frac{\partial^2 c_i}{\partial x^2} \quad (x_{i-1} < x < x_i; t > 0; i = 0, 1, \ldots, n) \tag{3.99a}$$

with the following non-dimensional initial conditions:

$$c_0(x, t = 0) = F_0(x) \quad (-l_0 = -x_{-1} < x < x_0 = 0) \tag{3.99b}$$

$$c_i(x, t = 0) = 0 \quad (x_{i-1} < x < x_i; i = 1, 2, \ldots, n) \tag{3.99c}$$

and with the following dimensionless interface and boundary conditions:

$$\left(\frac{\partial c_0}{\partial x}\right)_{x=-l_0} = 0 \quad (t > 0) \tag{3.99d}$$

$$\gamma_0 \left(\frac{\partial c_0}{\partial x}\right)_{x=0} = \gamma_1 \left(\frac{\partial c_1}{\partial x}\right)_{x=0} \quad (t > 0) \tag{3.99e}$$

$$-\gamma_0 \left(\frac{\partial c_0}{\partial x}\right)_{x=0} = \phi \left[\frac{c_0(0,t)}{\sigma_0} - \frac{c_1(0,t)}{\sigma_1}\right] \quad (t > 0) \tag{3.99f}$$

$$\gamma_i \left(\frac{\partial c_i}{\partial x}\right)_{x=x_i} = \gamma_{i+1} \left(\frac{\partial c_{i+1}}{\partial x}\right)_{x=x_i} \quad (i = 1, 2, \ldots, n-1; t > 0) \tag{3.99g}$$

$$\frac{c_i(x_i, t)}{\sigma_i} = \frac{c_{i+1}(x_i, t)}{\sigma_{i+1}} \quad (i = 1, 2, \ldots, n-1; t > 0) \tag{3.99h}$$

$$c_n(x = x_n = 1, t) = 0 \quad (t > 0) \tag{3.99i}$$

The development of the solution of Eq. (3.99a) according to the conditions (3.99b)–(3.99i) is presented in the study [61] in which the SOV method is still used to arrive at the following series solution:

$$c_i(x,t) = \sum_{m=1}^{\infty} A_m X_{im}(x) \exp\left(-\gamma_i \lambda_{im}^2 t\right) \quad (x_{i-1} \le x \le x_i; t \ge 0; i = 0, 1, \ldots, n) \tag{3.100}$$

where the n layer's eigenvalues are related among them by the relationship $\lambda_{0m}\sqrt{\lambda_0} = \lambda_{im}\sqrt{\lambda_i}$, with $i = 1, 2, \ldots, n$. A different method of solution based on a generalized integral transform is given in [62].

For Layer 0 the eigenfunction is represented by the expression:

$$X_{om}(x) = -\frac{1}{\tan(\lambda_{0m} l_0)} \cos(\lambda_{om} x) + \sin(\lambda_{om} x) \tag{3.101a}$$

The eigenfunctions of layers $i = 1, 2, \ldots, m$ are

$$X_{im}(x) = a_{im} \cos(\lambda_{im} x) + b_{im} \sin(\lambda_{im} x) \tag{3.101b}$$

for which $a_{i,m}$ and $b_{i,m}$ are constants associated with series term 'm' and Layer i. In detail, the constants of Layer 1 are:

$$a_{1m} = \frac{\sigma_1}{\sigma_0} X_{om}(0) + \frac{\gamma_0 \sigma_1}{\phi} \left(\frac{dX_{0m}}{dx}\right)_{x=0} \tag{3.102a}$$

$$b_{1m} = \frac{1}{\lambda_{1m}} \frac{\gamma_0}{\gamma_1} \left(\frac{dX_{0m}}{dx}\right)_{x=0} \tag{3.102b}$$

and the constants of the layers $i = 1, 2, \ldots, n$ are:

$$a_{im} = \frac{\sigma_i}{\sigma_{i-1}} \cos\left(\lambda_{im} x_{i-1}\right) X_{i-1m}(x_{i-1}) - \frac{1}{\lambda_{im}} \frac{\gamma_{i-1}}{\gamma_i} \sin(\lambda_{im} x_{i-1}) \left(\frac{dX_{i-1m}}{dx}\right)_{x=x_{i-1}} \tag{3.103a}$$

$$b_{im} = \frac{\sigma_i}{\sigma_{i-1}} \sin\left(\lambda_{im} x_{i-1}\right) X_{i-1m}(x_{i-1}) + \frac{1}{\lambda_{im}} \frac{\gamma_{i-1}}{\gamma_i} \cos(\lambda_{im} x_{i-1}) \left(\frac{dX_{i-1m}}{dx}\right)_{x=x_{i-1}} \tag{3.103b}$$

In Eq. (3.100), the constant A_m may still be evaluated by using Eq. (3.91) as the initial drug concentration is different from zero only in the coating. For the special case of a Layer 0 uniform initial distribution, $F_0(x) = 1$, it may be taken as $A_m = -1/(\sigma_0 N_m \lambda_{om})$, where the norm, N_m, is defined by:

$$N_m = \sum_{i=0}^{n} \frac{1}{2\sigma_i} \left\{ x X_{im}^2 + \frac{1}{\lambda_{im}^2} \left[x \left(\frac{dX_{im}}{dx}\right)^2 - X_{im} \frac{dX_{im}}{dx} \right] \right\} \Bigg|_{x_{i-1}}^{x_i} \tag{3.104}$$

And to close the solution set, the eigenvalues of Layer 0, λ_{0m}, may be determined by evaluating the roots of the transcendental equation (multi-layer eigencondition):

$$a_{nm}\cos(\lambda_{nm}) + b_{nm}\sin(\lambda_{nm}) = 0 \tag{3.105}$$

where the coefficients a_{nm} and b_{nm} are given by Eqs. (3.103a) and (3.103b), respectively, for $i = n$, and $\lambda_{nm} = \lambda_{0m}\sqrt{\gamma_0/\gamma_n}$.

Once the drug concentration is known, the dimensionless drug mass per unit area, $\tilde{M}_i = M_i/(C_0 d^*)$, contained within each layer ($i = 0, 1, \ldots, n$), may be taken as (re-setting $\tilde{M}_i \to M_i$):

$$M_0(t) = \int_{-l_0}^{0} c_0(x,t)\,dx = -\sum_{m=1}^{\infty} \frac{A_m}{\lambda_{0,m}} \exp\left(-\gamma_0 \lambda_{0,m}^2 t\right) \tag{3.106a}$$

$$M_i(t) = \int_{x_{i-1}}^{x_i} c_i(x,t)\,dx = \sum_{m=1}^{\infty} A_m \frac{\exp\left(-\gamma_i \lambda_{im}^2 t\right)}{\lambda_{im}^2} \left[\left(\frac{dX_{im}}{dx}\right)_{x_{i-1}} - \left(\frac{dX_{im}}{dx}\right)_{x_i}\right] (i = 1, 2, \ldots, n) \tag{3.106b}$$

In the study [61] the multi-layered wall model is developed in which the stent coating and five layers of arterial wall are represented using the geometric and physical parameter values listed in Table 3.1, with a uniform initial concentration within the stent coating, and a membrane permeability value of $P = 10^{-6}$ cm^2 s^{-1}.

The dimensionless parameter groups are scaled by the penetration depth d^*, and so it is evaluated from Eq. (3.96) with an accuracy of p=2, i.e., 1%. See the study [61] for a detailed account of the relationship between penetration depth, time and accuracy. The results of that study are shown in Fig. 3.21, in which the dimensionless concentration profiles within each of the layers are plotted at representative times.

The drug is retained differently in each layer, which receives mass from the inner and transmits to the outer, in a cascade sequence, and that are completely damped out at the distance d^* which represents the outer domain boundary. It is interesting to note that the levels of concentration in layer 2 (intima) are nearly constant and can be higher than in the others at intermediate times. This is in agreement with the higher diffusivity D_2 and relatively small layer thickness l_2.

TABLE 3.1 The parameters used in the simulations for the coating and the wall layers. The penetration distance d^* estimates the wall bound, provides the thickness l_5 of the external layer and depends on the maximum simulated time.

	Coating (0)	Endothelium (1)	Intima (2)	IEL (3)	Media (4)	Adventitia (5)
$l_i = x_i - x_{i-1}$(cm)	5×10^{-4}	2×10^{-4}	10^{-3}	2×10^{-4}	2×10^{-2}	$d^* - x_4$
D_i(cm^2/s)	10^{-10}	8×10^{-9}	7.7×10^{-8}	4.2×10^{-8}	7.7×10^{-8}	12×10^{-8}
ϵ_i	0.1	5×10^{-4}	0.61	4×10^{-3}	0.61	0.85
k_i	1	1	1	1	1	1

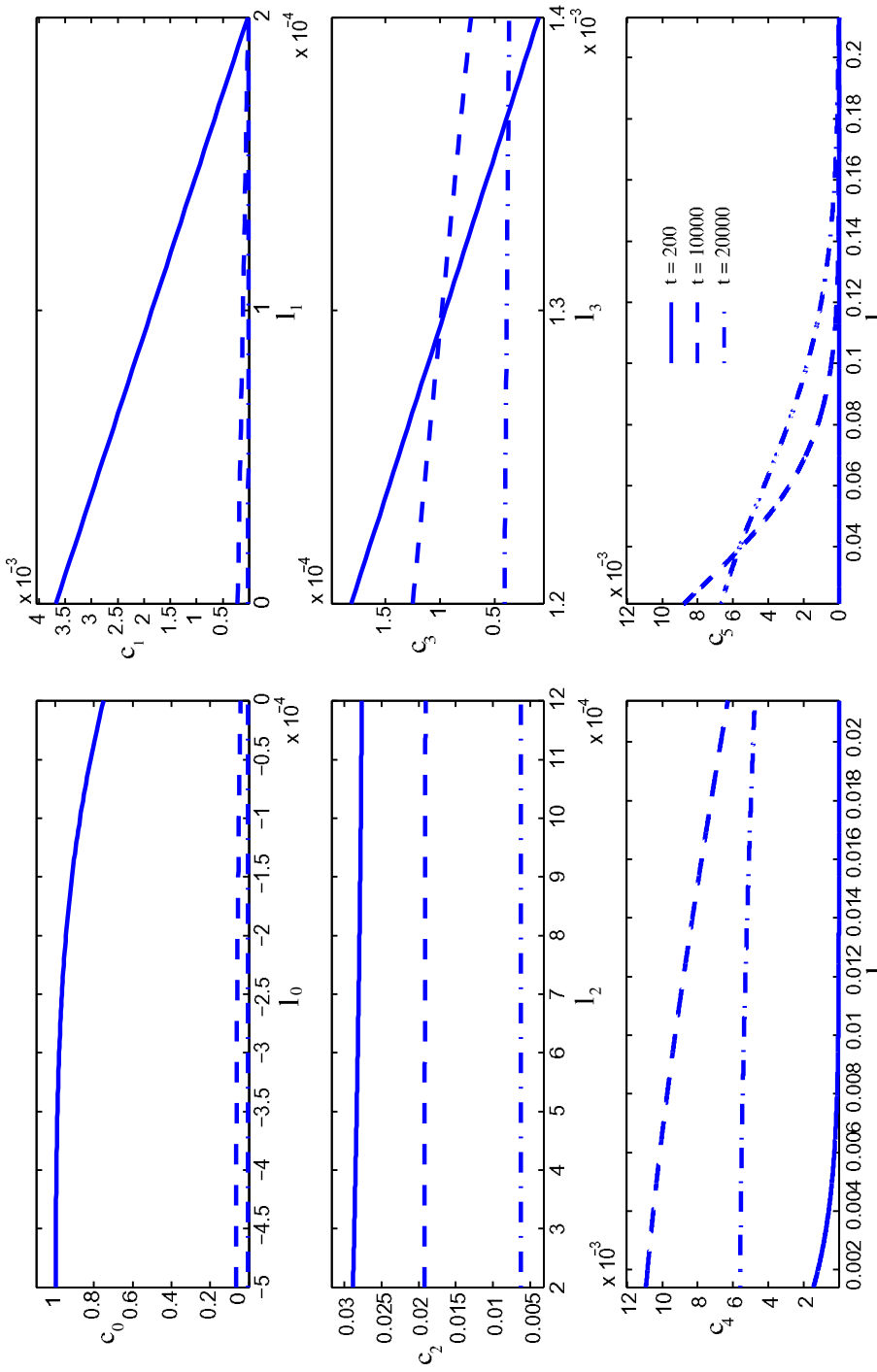

FIGURE 3.21 Concentration profiles in the six layers at three different times (in s) (note the different scale for coordinates and concentrations).

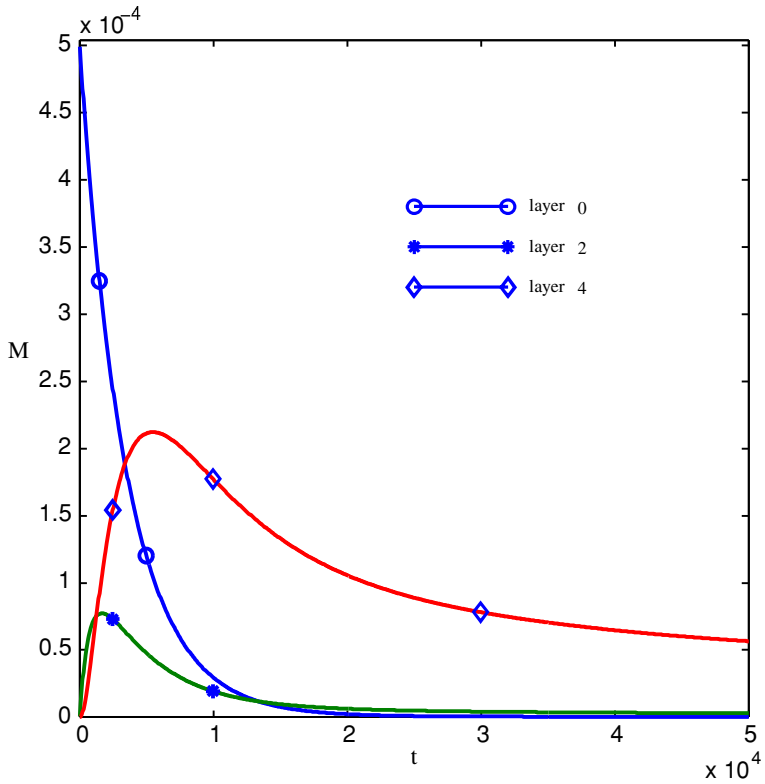

FIGURE 3.22 Dimensionless mass in the coating (layer 0), endothelium (layer 2) and media (layer 4) vs. time (in s). In the coating, mass is monotonically decreasing, while in the others there is a characteristic time at which the drug reaches a peak.

Due to the diffusive coefficient and to the porosity, the mass decreases exponentially in the coating and in layer (1) (innermost layers). However, in layers 2–5 the concentration experiences an initial build-up and then decays exponentially. This is very evident in the dimensionless mass contained in each layer, which is depicted in Fig. 3.22. In the outmost layer (5) the mass accumulates as the time proceeds. The simulation points out that the time of peak mass in the intima (layer 2) is at 1640 s ($\approx$ 27 min), in the media (layer 4) is 5460 s ($\approx$ 1 h: 30 min). The thin layers 1 and 3 retain a negligible mass due to their thickness, and the media is completely emptied after a time of about 57 days. At that time, all the mass is transferred to the external wall layer, with a slight mass loss. However, the therapeutic effects of DES is limited in the endothelium-media, while the residual drug in the outmost layer is considered lost.

3.7 CONCLUSION

The transport of drugs into biological media is a complex phenomenon that occurs over a range of time and length scales. Modeling of transport requires a deeper understanding not only of the solute and drug characteristics, but also of the physical structure of the biological

media. The porous media representation of the biological tissue in which the drug is carried allows for a continuum scale analysis of the interaction between drug and tissue, which may be based on relatively simple fundamental conservation laws. These lead to the ability to apply the analytical solutions of Nusselt, Schumann and Anzelius to the transient behavior of drug in a homogenous medium.

When, as often is the case, the biological tissue is not macroscopically homogenous, but rather is constituted from different discrete layers, a composite porous media representation of the tissue is likely to be used. An obvious and important application of the composite structure representation is the transport of drug from a stent through the wall of a blood vessel. Analytical solutions of different representations have been provided that allow for variability in application including the fluid wall model with pure diffusion, the fluid wall model with diffusion, advection and drug reaction and the diffusive multi-layered wall model.

References

[1] J.E. Sousa, P.W. Serruys, M.A. Costa, New frontiers in cardiology, drug-eluting stents: Part I. Circulation 107 (2003) 2274–2279.
[2] J.E. Sousa, P.W. Serruys, M.A. Costa, New frontiers in cardiology, drug-eluting stents: Part II. Circulation 107 (2003) 2382–2389.
[3] H. Hara, M. Nakamura, J.C. Palmaz, R.S. Schwartz, Role of stent design and coatings on restenosis and thrombosis, Advanced Drug Delivery Reviews 58 (2006) 377–386.
[4] W.H. Maisel, Unanswered questions – drug-eluting stents and the risk of late thrombosis, New England Journal of Medicine 356 (2007) 981–984.
[5] G. Pontrelli, F. de Monte, Mass diffusion through two-layer porous media: An application to the drug-eluting stent, International Journal of Heat and Mass Transfer 50 (2007) 3658–3669.
[6] J.M. Weiler, E.M. Sparrow, R. Ramazani, Mass transfer by advection and diffusion from a drug-eluting stent, International Journal of Heat and Mass Transfer 55 (2012) 1–7.
[7] N.I. Border, P.E. Buchwald, Ophthalmic drug design based on the metabolic activity of the eye: soft drugs and chemical delivery systems, AAPS Journal 7 (2005) 820–833.
[8] R. Avtar, D. Tandon, Modeling the drug transport in the anterior segment of the eye, European Journal of Pharmaceutical Sciences 35 (2008) 175–182.
[9] R. Manitz, W. Lucht, K. Strehmel, R. Weiner, R. Neubert, On mathematical modeling of dermal and transdermal drug delivery, Journal of Pharmaceutical Sciences 87 (1998) 873–879.
[10] M.R. Prausnitz, R. Langer, Transdermal drug delivery, Nature Biotechnology 26 (2008) 1261–1268.
[11] J.E. Rim, P.M. Pinsky, W.W. van Osdol, Multiscale modeling framework of transdermal drug delivery, Annals of Biomedical Engineering 37 (2009) 1217–1229.
[12] A.R.A. Khaled, K. Vafai, The role of porous media in modeling flow and heat transfer in biological tissues, International Journal of Heat and Mass Transfer 46 (2003) 4989–5003.
[13] Y. Davit, G. Debenest, B.D. Wood, M. Quintard, Modeling non-equilibrium mass transport in biologically reactive porous media, Advances in Water Resources 33 (2010) 1075–1093.
[14] F. Golfier, B.D. Wood, L. Orgogozo, M. Quintard, M. Bues, Biofilms in porous media: development of macroscopic transport equations via volume averaging with closure for local mass equilibrium conditions, Advances in Water Resources 32 (2009) 463–485.
[15] G.A. Truskey, F. Yuan, D.F. Katz, Transport Phenomena in Biological Systems, second ed., Pearson Prentice Hall Bioengineering, Lebanon, Indiana, USA, 2009.
[16] A. Bejan, Porous media, in: A. Bejan, A.D. Kraus (Ed.), Heat Transfer Handbook, Wiley, New York, 2003, pp. 1131–1180.
[17] D.A. Nield, A. Bejan, Convection in Porous Media, third ed., Springer, New York, 2006.
[18] M. Jakob, Heat Transfer, vol. 2, John Wiley & Sons, New York, 1957.

[19] M. Abramowitz, I.A. Stegun, Handbook of mathematical functions, in: Applied Mathematics Series, vol. 55, National Bureau of Standards, 1964.
[20] A.A. Rabah, S. Kabelac, A simplified solution of the regenerator periodic problem: the case for air conditioning, Forsch Ingenieurwes 74 (2012) 207–214.
[21] T.E.W. Schumann, Heat transfer: liquid flowing through a porous prism, Journal of the Franklin 208 (1929) 405–416.
[22] H.S. Carslaw, J.C. Jaeger, Conduction of Heat in Solids, second ed., Clarendon Press, London, 1959.
[23] A. Kuznetsov, An investigation of a wave of temperature difference between solid and fluid phases in a porous packed-bed, International Journal of Heat and Mass Transfer 37 (1994) 3030–3033.
[24] A. Kuznetsov, A perturbation solution for a nonthermal equilibrium fluid flow through a three-dimensional sensible heat storage packed bed, ASME Journal of Heat Transfer 118 (1996) 508–510.
[25] A. Kuznetsov, A perturbation solution for heating a rectangular sensible heat storage packed bed with a constant temperature at the walls, International Journal of Heat and Mass Transfer 40 (1997) 1001–1006.
[26] D.K. Tzou, Macro- to Microscale Heat Transfer, Taylor and Francis, New York, 1997.
[27] W.J. Minkowycz, A. Haji-Sheikh, K. Vafai, On departure from local thermal equilibrium in porous media due to a rapidly changing heat source: the Sparrow number, International Journal of Heat and Mass Transfer 42 (1999) 3373–3385.
[28] A. Haji-Sheikh, W.J. Minkowycz, Heat transfer analysis under local thermal non-equilibrium conditions, in: P. Vadàsz (Ed.), Emerging Topics in Heat and Mass Transfer in Porous Media From Bioengineering and Microelectronics to Nanotechnology, Springer, Dordrecht, 2008, 39–62.
[29] J. Crank, The Mathematics of Diffusion, second ed., Clarendon Press, Oxford, 1979.
[30] K.D. Cole, J.V. Beck, A. Haji-Sheikh, B. Litkouhi, Heat Conduction Using Green's Functions, second ed., CRC Press, Boca Raton, 2011.
[31] G. Pontrelli, F. de Monte, Modeling of mass dynamics in arterial drug-eluting stents, Journal of Porous Media 12 (2009) 19–28.
[32] L.M. Jiji, Heat Conduction, third ed., Springer-Verlag, Berlin, 2009.
[33] A. Haji-Sheikh, J.V. Beck, An efficient method of computing eigenvalues in heat conduction, Numerical Heat Transfer (Part B-Fundamentals) 38 (2000) 133–156.
[34] J.V. Beck, K.D. Cole, Improving convergence of summations in heat conduction, International Journal of Heat and Mass Transfer 50 (2007) 257–268.
[35] J.V. Beck, R. McMasters, K.J. Dowding, D.E. Amos, Intrinsic verification methods in linear heat conduction, International Journal of Heat and Mass Transfer 49 (2006) 2984–2994.
[36] S. Prabhu, S. Hossainy, Modeling of degradation and drug release from a biodegradable stent coating, Journal of Biomedical Materials Research, Part A 80A (2007) 732–741.
[37] S. Hossainy, S. Prabhu, A mathematical model for predicting drug release from a biodurable drug-eluting stent coating, Journal of Biomedical Materials Research, Part A 87A (2008) 487–493.
[38] S. Baek, A.R. Srinivasa, Modeling of the pH-sensitive behavior of a ionic gel in the presence of diffusion, International Journal of Non-Linear Mechanics 39 (2004) 1301–1318.
[39] P. Zunino, Multidimensional pharmacokinetic models applied to the design of drug-eluting stents, Cardiovascular Engineering: An International Journal 4 (2004) 181–191.
[40] D.V. Sakharov, L.V. Kalachev, D.C. Rijken, Numerical simulation of local pharmacokinetics of a drug after intravascular delivery with an eluting stent, Journal of Drug Targeting 10 (2002) 507–513.
[41] M.C. Delfour, A. Garon, V. Longo, Modeling and design of coated stents to optimize the effect of the dose, Siam Journal on Applied Mathematics 65 (2005) 858–881.
[42] C.J. Creel, M.A. Lovich, E.R. Edelman, Arterial paclitaxel distribution and deposition, Circulation Research 86 (2000) 879–884.
[43] G.A. Ateshian, M.H. Friedman, Integrative biomechanics: a paradigm for clinical applications of fundamental mechanics, Journal of Biomechanics 42 (2009) 1444–1451.
[44] G. Vairo, M. Cioffi, R. Cottone, G. Dubini, F. Migliavacca, Drug release from coronary eluting stents: a multidomain approach, Journal of Biomechanics 43 (2010) 1580–1589.
[45] R. Mongrain, I. Faik, R.L. Leask, J. Rodes-Cabau, E. Larose, O.F. Bertrand, Effects of diffusion coefficients and struts apposition using numerical simulations for drug eluting coronary stents, ASME Journal of Biomechanical Engineering 129 (2007) 733–742.

[46] M. Grassi, G. Pontrelli, L. Teresi, G. Grassi, L. Comel, A. Ferluga, L. Galasso, Novel design of drug delivery in stented arteries: a numerical comparative study, Mathematical Biosciences and Engineering 6 (2009) 493–508.
[47] F. Migliavacca, F. Gervaso, M. Prosi, P. Zunino, S. Minisini, L. Formaggia, G. Dubini, Expansion and drug elution model of a coronary stent, Computer Methods in Biomechanics and Biomedical Engineering 10 (2007) 493–508.
[48] M. Prosi, P. Zunino, K. Perktold, A. Quarteroni, Mathematical and numerical models for transfer of low-density lipoproteins through the arterial walls: a new methodology for the model set up with applications to the study of disturbed lumenal flow, Journal of Biomechanics 38 (2005) 903–917.
[49] C. Vergara, P. Zunino, Multiscale boundary conditions for drug release from cardiovascular stents, Multiscale Modeling & Simulation 7 (2008) 565–588.
[50] N. Yang, K. Vafai, Low-density lipoprotein (ldl) transport in an artery – a simplified analytical solution, International Journal of Heat and Mass Transfer 51 (2008) 497–505.
[51] M. Khakpour, K. Vafai, Critical assessment of arterial transport models, International Journal of Heat and Mass Transfer 51 (2008) 807–822.
[52] G. Pontrelli, A. Di Mascio, F. de Monte, Local mass non-equilibrium in arterial drug-eluting stents, WAMS 2012, The International Workshop on Applied Modeling and Simulation, Rome, Italy, 24–27 September, 2012.
[53] A. Kargol, M. Kargol, S. Przestalski, The Kedem-Katchalsky equations as applied for describing substance transport across biological membranes, Cellular and Molecular Biology Letters 2 (1997) 117–124.
[54] A. Kargol, Modified Kedem-Katchalsky equations and their applications, Journal of Membrane Science 174 (2000) 43–53.
[55] C.W. Hwang, D. Wu, E.R. Edelman, Physiological transport forces govern drug distribution for stent-based delivery, Circulation 104 (2001) 600–605.
[56] M. Khakpour, K. Vafai, Effects of gender-related geometrical characteristics of aortailiac bifurcation on hemodynamics and macromolecule concentration distribution, International Journal of Heat and Mass Transfer 51 (2008) 5542–5551.
[57] M.N. Özişik, Heat Conduction, second ed., John Wiley & Sons, New York, 1993.
[58] G. Meyer, R. Merval, A. Tedgui, Effects of pressure-induced stretch and convection on low-density lipoprotein and albumin uptake in the rabbit aortic wall, Circulation Research 79 (1996) 532–540.
[59] L. Ai, K. Vafai, A coupling model for macromolecule transport in a stenosed arterial wall, International Journal of Heat and Mass Transfer 49 (2006) 1568–1591.
[60] M. Khakpour, K. Vafai, A comprehensive analytical solution of macromolecular transport within an artery, International Journal of Heat and Mass Transfer 51 (2008) 2905–2913.
[61] G. Pontrelli, F. de Monte, A multi-layer porous wall model for coronary drug-eluting stents, International Journal of Heat and Mass Transfer 53 (2010) 3629–3637.
[62] C. Liu, W.P. Ball, J.H. Hellis, An analytical solution to the one-dimensional solute advection-dispersion equation in multi-layer porous media, Transport in Porous Media 30 (1998) 25–43.